POLYTECHNIC INSTITUTE OF BROOKLYN

GAS TURBINE LABORATORY

DEPARTMENT OF MECHANICAL ENGINEERING

TECHNICAL REPORT No. 1 JULY, 1954

ANALYSIS OF TIP-CLEARANCE FLOW IN TURBOMACHINES

BY

CHUNG HUA WU AND WEN WU

PREPARED UNDER
CONTRACT NONR 839(04)
NR-062-172
OFFICE OF NAVAL RESEARCH
U. S. DEPARTMENT OF THE NAVY
WASHINGTON, D. C.

ABSTRACT

A basic analysis of the blade tip flow phenomena is presented. The analysis is based on a steady relative flow of a viscous incompressible fluid. A rotating cylindrical coordinate system which moves with the blade at the same speed is used.

An order-of-magnitude analysis reduces the basic equations to a set of simplified equations for both low and high Reynolds number. Expressions are given for the determination of the distributions of pressure and velocity in the clearance space and the mass flow across the tip clearance space. The computation of the velocity distribution is relatively simple and three methods of solution for the pressure distribution are presented.

TABLE OF CONTENTS

INTRODUCTION

Because of the relative motion between the rotating blades and the stationary casing wall in the turbomachines, a clearance space has to be provided to avoid physical rubbing and consequent damaging of the machine. The existence of the tip-clearance complicates greatly the internal fluid flow in turbomachines. Briefly, the tip-clearance flow is a three-dimensional flow problem. The tip-clearance flow has long been considered to be one of the factors responsible for internal losses in trubomachines[1]*, although opinion of its importance varies. The loss due to tip clearance flow has also been known to be closely associated with the secondary-flow loss and the annulus-wall loss. The tip-leakage flow is due to the pressure difference across the blade-tip section and the relative motion between the blade and the bounding wall and is transverse to the main-flow direction. The secondary-flow is due to the pressure difference across the space between two adjacent blades and is also transverse to the main-flow direction. The annulus wall loss is due to the boundary layer at the wall. All these losses are originated within the boundary layers of the casing wall surfaces.

Of course, the tip-clearance should be kept as small as possible. But the "warm clearance" varies over a wide range under different operating conditions[2]. It is therefore advisable to provide a liberal clearance in order to avoid rubbing under most unfavorable conditions. "Shrouding" of blade tips decreases the tip-loss but introduces other

*Number in parenthesis refers to the reference number given at the end of the report.

losses.[3] In one compressor test,[4] it has been found that the compressor with shrouded blades has both lower pressure coefficient and overall compressor efficiency than those of a compressor without shrouding. However, this single test cannot be taken as conclusive.[5] Others claim shrouding will eliminate the induced secondary flow loss which is caused by the moving-wall. It seems that shrouding only changes the tip-loss problem to a different one instead of being a simple remedy. Our study is confined to free tip blades.

The purpose of this investigation is to make a basic study of the flow phenomenon pattern around the tip-clearance space, to analyze the design and operating parameters which control this clearance flow, and to determine its effect on the machine performance. It is hoped that out of a thorough understanding of the tip-flow phenomena, the limit of the permissible clearance may be calculated. This report presents the initial theoretical study of this problem.

A BRIEF SURVEY OF PREVIOUS INVESTIGATIONS

Up to date, complete treatment of the tip-loss problem is not available, even though it has attracted attention in the steam-turbine development as early as 1905.[6] The available information regarding the tip-loss problem can be summarized into the following different groups:

Theoretical Investigation

Betz[7] made the first theoretical investigation of the tip-loss in the Kaplan water turbines by applying the lifting line theory to a simplified two-dimensional rectilinear cascade.[8] Later, Sedille also using lifting-line theory, treated the tip-loss problem in the

axial compressor. The results obtained by this method were found much larger than those observed in practice. The discrepancy was attributed by Sedille to the resistances which opposed the flow in the tip clearance space which prevails in the actual machines but are neglected in the analyses. These resistances included annulus wall boundary layers, blade thickness, radial flow of blade boundary layers, local turbulence, etc.

Semi-Empirical Estimation of Tip-Loss

In order to meet the urgent practical need in design, various semi-empirical formulae have been suggested to estimate the tip-loss in turbomachines. These formulae were chiefly based upon simplified theoretical analyses under certain assumptions or limitations. The empirical constants have to be evaluated from test data. This group of investigators includes Meldahl,[9] Traupel[10] and Fickert.[11] Their suggested formulae respectively are:

Investigators	Suggested Formulae	Assumptions and Limitation
(1) Meldahl(1941)	End Losses: $L_e = .1011 + 4.667(\frac{s}{c})$ Where s = tip-clearance, c = blade-chord	(1) Based upon lift-line theory and 2-Dimensional blades cascade (2) Good only for single stage reaction turbine (3) Including secondary flow loss

(2) Traupel (1942) Tip Loss:

$$L_t = K\left(\frac{A_c}{A_a}\right)\frac{\sqrt{\left(\frac{3}{t}\right)\Delta U}}{\sin\alpha}$$

Where: K = Flow Coeff.

A_c = clearance area

A_a = annular area

t = pitch

ΔU = change of tangential component of velocity

α = cascade angle

(1) Based on Bernoulli's equation

(2) Flow coeff. 'K' has to be evaluated from test data

(3) K has different values for rotor and stator

(3) Fickert (1943) Volumetric eff.

$$\eta = \frac{1}{1 + 4\mu\left[\frac{s/D_a}{1-\left(\frac{D_h}{D_a}\right)^2}\right]\sigma^{-1/2}}$$

Where: μ = coeff. of contraction

D_a = casing diameter

D_h = hub "

σ = throttling coeff.

(1) Based upon Bernoulli's equation

(2) Cooff of contraction 'μ' has to be evaluated from test data

Experimental Investigation

In axial compressor tests the variation of compressor efficiency with tip-clearance was obtained by Sedille,[8] Ruden[12] and Lindsay.[13] These results show a nearly linear relationship between the efficiency drop and the tip-clearance increase. However, neither detailed

explanations nor theory were advanced from those testing results.*

Qualitative Investigation of the Moving-Wall Effect

Recently, efforts have been made to understand the moving-wall effect on the clearance flow. This is an attempt to separate one factor from others affecting the clearance flow. Ainley and Jeffs[5] concluded from their compressor test that the rotating drum drags along the adjacent fluid through the tip-clearance space in addition inducing a secondary flow. Carter[3] indicated that, in the case of a compressor, the clearance flow will be augmented by the moving wall and that the induced secondary flow was the "scraping effect' of the moving-wall; but in the turbine, the clearance flow will be reduced by the moving wall. Both the 'scraping effect' and the reduced clearance flow in the turbine were confirmed by Hansen, Herzig, Costello, in their smoke visualization experiment in a cascade tunnel.[15] But their results regarding the clearance flow in the compressor were in contradiction to Carter's prediction. Their experiments show that the moving wall has a tendency to diminish the clearance flow rather than to promote it. This point needs clarification by further experiments, and will be one of the objects to be studied in the experimental part of this research project.

In hydraulic turbomachines, such as pumps and marine ducted propellers, the so-called "vortex cavitation" has been observed.[16] Fluid, passing through the tip clearance, forms the tip vortex. At the

* It has come to our attention very recently that a report[14] on Tip-Loss has been published in Germany in 1952. However, that report is not yet available to us at the present time.

center of this vortex, cavities are produced. These cavities appear and form a nearly continuous core which starts at about the leading edge of the blade and extends downstream. The magnitude of the cavities seems to depend upon the tip-clearance.

From the preceding survey of the previous investigations, we may conclude that:

(1) Tip-clearance flow contributes considerable loss in turbomachines, especially when the clearance is large.

(2) Tip-clearance flow is affected by factors, such as blade-tip thickness, blade loading (especially loading conditions near tip section), relative motion effect, annulus wall boundary layer, blade boundary layer, etc. Therefore, it is a 3-D'al boundary layer problem.

PRELIMINARY STUDY OF TIP LOSS PROBLEM

When a lifting surface (either a wing or a blade) is placed in line with a passing fluid, a true 2-D'al flow can be achieved only if the lifting surface has an infinite span. However, in reality, the lifting surface has only finite span, therefore, 3-D'al flow phenomena prevails. In the case of a wing, the lifting surface has a free end, or tip. The fluid on the pressure surface tries to flow to the suction surface over the free tip. Consequently, a trailing vortex sheet is formed behind the wing. (Fig. 1). The vortex sheet causes the induced drag of the wing. In the case of a cascade of blades which are attached to end walls, secondary flow is developed both in the end wall boundary layer [17] and in the main flow (passage vortex) [18]. The boundary layer fluid on the pressure surface of one blade flows to the suction surface of its adjacent blade along the end wall. (Fig. 2). Downstream of the cascade,

a trailing vortex sheet again is formed. If "clearance" exists between the blade tip and the end wall (consider for the time being that the end wall is stationary), both the secondary flow in the end wall and the trailing vortices will still be present but with different magnitude. Because of the clearance, the fluid on the pressure surface will tend to flow to the suction surface of the same blade (since the passage is shorter and the pressure difference is the same) instead of to the suction surface of the adjacent blade. (Fig. 3). Due to this clearance flow, the pressure gradient between the pressure and the suction surfaces will no longer be the same as that when there is no clearance. Therefore, the secondary flow will somewhat decrease in strength. No doubt, this rearrange of flow pattern in the boundary layer will, in turn, influence the flow in the main stream. It may be noted here that both the secondary flow and the clearance flow are in a plane transverse to the main-flow direction.

Now, let the end wall move, so we can have a condition corresponding to the actual one in turbomachines. In the compressor, the pressure surface is leading in the moving direction and in the turbine, the suction surface is leading. For the time being, let us agree that the moving wall, due to viscous effect, will drag along the fluid with it when it passes over the blade-tip. Thus, in the compressor, because the wall (relative motion) moves in the same direction to that of the pressure difference (hence in the direction of the clearance flow) across the blade tip, it is expected that the clearance flow will be augmented (Fig. 4) while in the turbine, the wall moves in an opposite direction to that of the pressure difference, it is expected that the clearance flow will be reduced (Fig. 5).

It seems that it is necessary to point out that there is a difference between the amount of fluid flow through the tip-clearance and the strength of the vortex formed due to this tip-clearance flow. The amount of fluid-flow through the tip-clearance, as will be seen later, depends upon both the pressure gradient across the blade tip-section and the moving wall velocity. But the vortex strength depends only upon the pressure gradient across the blade tip-section. There are two extreme cases: (a) For stationary wall (zero velocity) and large pressure gradient, the tip-clearance vortex will be the strongest. (b) For large moving wall velocity and zero pressure gradient, there will be no tip-clearance vortex and the amount of fluid flow may be or may not be greater than that in case (a). In an actual machine, the situation for the vortex strength and the amount of fluid flow will be somewhere between cases (a) and (b). The moving wall, of course, tends to minimize the pressure gradient across the two sides of the blade when it drags the high-pressure fluid from one side to the low pressure region of the other side of the blade.

Because the flow in the boundary layer is primarily determined by the main flow, all the factors which affect the main flow will affect the flow in the boundary layer. The boundary layer flow condition in turn affects the tip-clearance flow. Therefore, the tip clearance flow is closely related to the main flow. The final forms of the main flow influence are manifested by the blade loading, casing wall boundary layer, relative motion effect, etc., as mentioned before. If these conditions prevailing outside the clearance space remain the same, the flow through the tip-clearance can be expected to be the same even though the main flow could be of different patterns

for different designs. Since the main flow in the turbomachine has many natures (19) on the one hand, and the lack of full knowledge regarding the three dimensional boundary layer flow (in this case, it will be secondary flow) on the other hand, it seems unwise to attempt to solve the tip-clearance problem together with the boundary layer flow and the main flow, but rather to assume conditions outside the clearance space and try to solve it accordingly. In other words, the boundary conditions of tip-clearance flow are not evident by themselves. They are related to the secondary flow and hence the main flow.

So far we consider the blade tip is inside the casing-wall boundary layer. In other words, we have considered only the case that the "warm clearance" is less than the thickness of the boundary layer of the adjacent casing wall. This will be true for most conditions, at least for later-stage rotors and stators in the compressor. In the following, we will concentrate our analysis on this assumption. Fortunately, for the case when the blade tip is outside of the boundary layer, the problem is much simpler to handle. Because both viscous effect and the relative motion effect can be ignored when the tip is outside of the boundary layer (Fig. 6), then the problem can be approached by the conventional lifting-line theory.

SYMBOLS

The following symbols are used in this report:

A = Coefficient of cosines of the velocity Fourier series

B = Coefficient of sines of the velocity Fourier series

C = Airfoil chord length - ft.

D = $(R^2 + c^2 \tan^2\beta + 2cR\tan\beta \sin\psi) + (2c\ell)(R\cos\psi + R\tan\beta\sin\psi + c\tan^2\beta) + c^2 \sec^2\beta\, \ell^2$ - ft.

L = Characteristic length of the turbomachine, either the blade chord or the blade height - ft.

M = $\left[A(1+\ell)cR\tan\beta(D+c^2)\right]\sin\psi - \left[A c\ell R(D-c^2)\right]\cos\psi - 2R^2 D\cos 2\psi + \left[\frac{D^3}{c^2} - c^2 D - 2(D-c^2)c^2\chi^2 + 2(D+c^2)(1+\ell)^2 c^2\tan^2\beta + 2c^2R^2\right]$ - ft.^{4}

Q = Rate of mass flow lb(M)/sec.

R = Radius in ξ'-η' plane (figure 14)

R' = Distance between point P and origin O (figure 14)

Re = Reynolds number - $\frac{W_0 L}{\nu}$

$\bar{V}$ = Absolute velocity of the fluid - ft./sec.

$\bar{W}$ = Relative velocity of the fluid - ft./sec.

a = radius of the transformed circle in ξ-η plane (figure 13B)

b = distance between point on the circle and origin O (figure 13B)

c = Constant of Joukowsky's transformation equation

i = Imaginary unit

l = component of MO in ξ direction in % of c (figure 13B)

m = Distance between M and O (figure 13B)

p = pressure lb(F.)/ft.^{2}

$q_0 = \frac{1}{2}\rho_0 W_0^2$ "

r = Radial distance in the cylindrical coordinates

r_c = Radial distance of the casing wall - ft.

r_h = Radial distance of the hub - ft.

r_t = Radial distance of the blade tip - ft.

s = Tip-clearance - in (or ft.)

t = Time - second

W_o = Relative velocity of the inlet fluid - ft/sec.

W_r, W_φ, W_z = Relative velocity components in r, φ and z direction respectively - ft/sec.

$x = z' + y'$

$y = \lambda r_t \varphi$ - distance in the tangential direction - ft.

z = Axial distance in the cylindrical coordinates

z' = Horizontal component in y' - z' plane (figure 13A)

α = Angle of attack of the inlet relative fluid - deg.

β = Angle between MN and z - axis (figure 13B) - deg.

δ = Angle between Mo and z - axis (figure 13B) - deg.

$\epsilon = \frac{z}{r_t}$

$\zeta = z + i\eta$ (figure 13B)

$\eta = \frac{z}{s}$

θ = Angle between OP and z -axis (figure 14)

$\lambda = \frac{r_c}{r_t}$ for rotor, $= \frac{r_h}{r_t}$ for stator

μ = Viscosity of fluid - lb(F)-sec/ft.^{2}

ν = Kinematic viscosity of fluid = $\frac{\mu}{\rho}$ - ft.^{2}/sec.

z = Radius distance from the blade tip inside the clearance space - in (or ft.)

ρ = density of fluid - lb.(M)/sec.

$\sigma = \frac{c}{t_t}$

φ = Angular displacement in the cylindrical coordinates - deg.

χ = Blade cascade stagger angle - deg.

ψ = Angle between PM and z -axis (figure 14) - deg.

ω = Rotating speed of the turbomachine - rad./sec.

Subscripts

a = At the contour of the airfoil section

c = Casing wall

h = Hub

t = Blade tip

r, φ, z = In the radial, tangential and axial directions of the cylindrical coordinates respectively.

BASIC EQUATIONS

The three-dimensional flow of a viscous incompressible fluid is governed by the following set of the basic laws of fluid mechanics. From the principle of conservation of matter,

$$\frac{\partial \rho}{\partial t} + \rho \nabla \cdot \bar{V} = 0 \tag{1}$$

From Newton's second law of motion,

$$\rho \frac{D\bar{V}}{Dt} = -\nabla P + \mu \nabla^2 \bar{V} \tag{2}$$

or

$$\frac{\partial \bar{V}}{\partial t} + (\bar{V} \cdot \nabla)\bar{V} = -\frac{1}{\rho}\nabla P + \nu \nabla^2 \bar{V} \tag{2a}$$

Since the absolute motion of fluid flow in a turbomachine is generally unsteady while the relative motion with respect to the blade is essentially steady, the preceding equations are further expressed in terms of the relative velocity W, which is related to the absolute velocity by the relation,

$$\bar{V} = \bar{W} + \bar{\omega} \times \bar{r} \tag{3}$$

In equation (3) $\bar{\omega}$ is the angular velocity of the blade about the z -axis) and $\bar{r}$ is the radius vector measured from the z - axis.

Now, for the blade rotating at a constant velocity $\bar{\omega}$ about the z-axis,

$$\frac{D\bar{V}}{Dt} = \frac{D\bar{W}}{Dt} - \omega^2 \bar{r} + 2\bar{\omega} \times \bar{W} \tag{4}$$

But

$$\frac{D\bar{W}}{Dt} = \frac{\partial \bar{W}}{\partial t} + (\bar{W} \cdot \nabla)\bar{W} = \frac{\partial \bar{W}}{\partial t} + \frac{1}{2}\nabla W^2 - \bar{W} \times (\nabla \times \bar{W}) \tag{4a}$$

When the preceding relations are used, equations (1) and (2) become (assuming steady relative flow),

$$\nabla \cdot \bar{W} = 0 \tag{5}$$

and

$$\frac{1}{2}\nabla W^2 - \bar{W} \times (\nabla \times \bar{W}) - \omega^2 \bar{r} + 2\bar{\omega} \times \bar{W} = -\frac{1}{\rho}\nabla p + \nu \nabla^2 \bar{V} \tag{6}$$

Since the boundary walls of a turbomachine are surfaces of revolution, a relative cylindrical coordinate system r, φ and z with φ measured with respect to the rotating blade and rotating with angular speed ω about the z-axis is employed. Then equation (5) becomes

$$\frac{1}{r}\frac{\partial}{\partial r}(r W_r) + \frac{1}{r}\frac{\partial W_\varphi}{\partial \varphi} + \frac{\partial W_z}{\partial z} = 0 \tag{7}$$

and equation (6) gives

(a) in radial direction:

$$W_r \frac{\partial W_r}{\partial r} + \frac{W_\varphi}{r}\frac{\partial W_r}{\partial \varphi} + W_z \frac{\partial W_r}{\partial z} - \frac{W_\varphi^2}{r} - \omega^2 r - 2\omega W_\varphi = -\frac{1}{\rho}\frac{\partial p}{\partial r} + \nu\left(\frac{\partial^2 W_r}{\partial r^2} + \frac{1}{r}\frac{\partial W_r}{\partial r} + \frac{1}{r^2}\frac{\partial^2 W_r}{\partial \varphi^2} + \frac{\partial^2 W_r}{\partial z^2} - \frac{W_r}{r^2} - \frac{2}{r^2}\frac{\partial W_\varphi}{\partial \varphi}\right) \tag{8a}$$

(b) in circumferential direction:

$$W_r \frac{\partial W_\varphi}{\partial r} + \frac{W_\varphi}{r}\frac{\partial W_\varphi}{\partial \varphi} + W_z \frac{\partial W_\varphi}{\partial z} + \frac{W_r W_\varphi}{r} + 2\omega W_r = -\frac{1}{\rho}\frac{\partial p}{r\partial \varphi} + \nu\left(\frac{\partial^2 W_\varphi}{\partial r^2} + \frac{1}{r}\frac{\partial W_\varphi}{\partial r} + \frac{1}{r^2}\frac{\partial^2 W_\varphi}{\partial \varphi^2} + \frac{\partial^2 W_\varphi}{\partial z^2} - \frac{W_\varphi}{r^2} + \frac{2}{r}\frac{\partial W_r}{\partial \varphi}\right) \tag{8b}$$

(c) in axial direction

$$W_r \frac{\partial W_z}{\partial r} + \frac{W_\varphi}{r}\frac{\partial W_z}{\partial \varphi} + W_z \frac{\partial W_z}{\partial z} = -\frac{1}{\rho}\frac{\partial p}{\partial z} + \nu\left(\frac{\partial^2 W_z}{\partial r^2} + \frac{1}{r}\frac{\partial W_z}{\partial r} + \frac{1}{r^2}\frac{\partial^2 W_z}{\partial \varphi^2} + \frac{\partial^2 W_z}{\partial z^2}\right) \tag{8c}$$

Although equations (7), (8a), (8b), and (8c) give four independent equations for the solution of four unknowns, W_r, W_φ, W_z & p there is yet no mathematical methods available for an exact solution of these equations. In the following, the usual procedure of an order-of-magnitude analysis is used to obtain a set of simplified equations for an approximate solution of the problem.

SIMPLIFIED EQUATIONS

We first transform equations (7) and (8) into dimensionless forms. Let the representative velocity be W_o, which is the relative velocity of approach to the blade just outside the boundary layer at the wall. Let the representative length be L, which may be either the radial length of the blade or the chord of the tip section of the blade. Then the equations are made dimensionless by introducing the following dimensionless variables

$$r' = \frac{r}{L}, \qquad z' = \frac{z}{L}, \qquad W_r' = \frac{W_r}{W_o}, \qquad W_\varphi' = \frac{W_\varphi}{W_o},$$

$$W_z' = \frac{W_z}{W_o}, \qquad \omega' = \frac{\omega L}{W_o}, \qquad p' = \frac{p}{\rho W_o^2}$$

Equations (7) and (8) then become

$$\frac{1}{r'}\frac{\partial}{\partial r'}(r' W_r') + \frac{1}{r'}\frac{\partial W_\varphi'}{\partial \varphi} + \frac{\partial W_z'}{\partial z'} = 0 \qquad (9)$$

$$W_r'\frac{\partial W_r'}{\partial r'} + \frac{W_\varphi'}{r'}\frac{\partial W_r'}{\partial \varphi} + W_z'\frac{\partial W_r'}{\partial z'} - \frac{W_\varphi'^2}{r'} - \omega'^2 r' - 2\omega' W_\varphi'$$

$$= -\frac{\partial p'}{\partial r'} + \frac{1}{Re}\left\{\frac{\partial^2 W_r'}{\partial r'^2} + \frac{1}{r'}\frac{\partial W_r'}{\partial r'} + \frac{1}{r'^2}\frac{\partial^2 W_r'}{\partial \varphi^2} + \frac{\partial^2 W_r'}{\partial z'^2} - \frac{W_r'}{r'^2} - \frac{2}{r'^2}\frac{\partial W_\varphi'}{\partial \varphi}\right\} \qquad (10a)$$

$$W_r'\frac{\partial W_\varphi'}{\partial r'} + \frac{W_\varphi'}{r'}\frac{\partial W_\varphi'}{\partial \varphi} + W_z'\frac{\partial W_\varphi'}{\partial z'} + \frac{W_r' W_\varphi'}{r'} + 2\omega' W_r'$$

$$= -\frac{\partial p'}{r'\partial \varphi} + \frac{1}{Re}\left\{\frac{\partial^2 W_\varphi'}{\partial r'^2} + \frac{1}{r'}\frac{\partial W_\varphi'}{\partial r'} + \frac{1}{r'^2}\frac{\partial^2 W_\varphi'}{\partial \varphi^2} + \frac{\partial^2 W_\varphi'}{\partial z'^2} - \frac{W_\varphi'}{r'^2} + \frac{2}{r'^2}\frac{\partial W_r'}{\partial \varphi}\right\}$$

(10b)

$$W_r' \frac{\partial W_z'}{\partial r'} + \frac{W_\varphi'}{r'} \frac{\partial W_z'}{\partial \varphi} + W_z' \frac{\partial W_z'}{\partial z'}$$

$$= -\frac{\partial p'}{\partial z'} + \frac{1}{Re}\left(\frac{\partial^2 W_z'}{\partial r'^2} + \frac{1}{r'} \frac{\partial W_z'}{\partial r'} + \frac{1}{r'^2} \frac{\partial^2 W_z'}{\partial \varphi^2} + \frac{\partial^2 W_z'}{\partial z'^2} \right) \quad (10c)$$

where $$R_e = \frac{W_c L}{\nu} \quad (11)$$

Now, r', z', W_φ', W_z', p' are of the same order and taken to be of order 1. The dimensionless tip-clearance s' (= s/L) is small of the first order, the same as the dimensionless boundary-layer thickness along the wall ξ' (= $\bar{\delta}$/L). They belong to the next smaller order than 1 and are indicated by $O(\delta')$. W_r' also has the order of δ'. Then, because

$$W_r' = \int_{r_t'}^{r_c'} \frac{\partial W_r'}{\partial r'} dr' = o(\delta')$$

$\partial W_r'/\partial r'$ is of the order 1. On the other hand, $\partial W_z'/\partial z'$ and $\frac{1}{r'} \partial W_\varphi'/\partial \varphi$ are of the order 1 (except at the bounding wall and the blade tip surface). Based on these orders of magnitudes, we found the order of magnitudes of all other terms in the quations and they are listed below:

$$o\left(\frac{1}{\delta'^2}\right) : - \quad \frac{\partial^2 W_\varphi'}{\partial r'^2}, \quad \frac{\partial^2 W_z'}{\partial r'^2}.$$

$$o\left(\frac{1}{\delta'}\right) : - \quad \frac{\partial W_\varphi'}{\partial r'}, \quad \frac{\partial W_z'}{\partial r'}, \quad \frac{\partial^2 W_r'}{\partial r'^2}$$

$$o(1) : - \quad \frac{\partial W_r'}{\partial r'}, \quad \frac{\partial W_\varphi'}{\partial z'}, \quad \frac{1}{r'} \frac{\partial W_z'}{\partial \varphi}, \quad \frac{1}{r'^2} \frac{\partial^2 W_\varphi'}{\partial \varphi^2}, \quad \frac{1}{r'^2} \frac{\partial^2 W_z'}{\partial \varphi^2},$$

and $$\frac{\partial^2 W_z'}{\partial z'^2}$$

$$o(\delta') : - \quad \frac{1}{r'} \frac{\partial W_r'}{\partial \varphi}, \quad \frac{\partial W_r'}{\partial z'}, \quad \frac{1}{r'^2} \frac{\partial^2 W_r'}{\partial \varphi^2}, \quad \frac{\partial^2 W_r'}{\partial z'^2}.$$

When these orders of magnitudes are used, and a term of order (δ') is omitted, the continuity equation (9) becomes

$$\frac{\partial W_r'}{\partial r'} + \frac{1}{r'}\frac{\partial W_\varphi'}{\partial \varphi} + \frac{\partial W_z'}{\partial z'} = 0 \qquad (12)$$

The relative importance of the various terms in equations (10) depend, however, on the order of magnitude of the Reynolds number.

For fluids of small viscosity, such as air and water at ordinary temperature and pressure, the characteristic Reynolds number is usually large and is in the order of $(1/\varepsilon'^2)$. For other fluids, such as lubricating oil and some liquid chemicals, ν is a hundred times greater and, especially with relatively small characteristic length L, the Reynolds number is of the order of $(1/\delta')$. The following simplified equations are therefore given, for these two orders of magnitude of the Reynolds number respectively.

Case I. Reynolds number of order of $1/\delta'$. In this case, equations (10) reduce to

$$\frac{\partial p'}{\partial r'} = \frac{W_\varphi'^2}{r'} + \omega'^2 r' + 2\omega' W_\varphi' + \frac{1}{Re}\frac{\partial^2 W_r'}{\partial r'^2} \qquad (13a)$$

$$\frac{1}{r'}\frac{\partial p'}{\partial \varphi} = \frac{1}{Re}\frac{\partial^2 W_\varphi'}{\partial r'^2} \qquad (13b)$$

$$\frac{\partial p'}{\partial z'} = \frac{1}{Re}\frac{\partial^2 W_z'}{\partial r'^2} \qquad (13c)$$

In equation (13a), we see that the viscous term is of the same order of magnitude as the inertia term. They both contribute to the radial pressure gradient.

In each of equations (13b) and (13c), only one viscous term predominates and essentially determines the circumferential and axial pressure gradient respectively.

It is noted that the terms on the right-hand side of equation (13a) are of the order of 1, while those on the right-hand side of equations (13b) and (13c) are of the order of $1/\delta'$. Therefore, the pressure gradient in the radial direction is much smaller than the pressure gradients in the other two directions. In other words, only equations (13b) and (13c) have to be considered in this case.

Case II. Reynolds number of order of $1/\delta'^2$. In this case equation (10) reduces to

$$\frac{\partial p'}{\partial r'} = \frac{(W_\varphi' + \omega' r')^2}{r'} = \frac{V_\varphi'^2}{r'} \tag{14a}$$

$$\frac{1}{r'}\frac{\partial p'}{\partial \varphi} = \frac{1}{Re}\frac{\partial^2 W_\varphi'}{\partial r'^2} - \left(W_r'\frac{\partial W_\varphi'}{\partial r'} + \frac{W_\varphi'}{r'}\frac{\partial W_\varphi'}{\partial \varphi} + W_z'\frac{\partial W_\varphi'}{\partial z'}\right) \tag{14b}$$

$$\frac{\partial p'}{\partial z'} = \frac{1}{Re}\frac{\partial^2 W_z'}{\partial r'^2} - \left(W_r'\frac{\partial W_z'}{\partial r'} + \frac{W_\varphi'}{r'}\frac{\partial W_z'}{\partial \varphi} + W_z'\frac{\partial W_z'}{\partial z'}\right) \tag{14c}$$

The inertia term now predominates in the right-hand side of equation (14a), which is recognized as the "simplified-radial-equilibrium equation.

It is noted that in this case all terms that appear on the right-hand side of the three equations are of the same order of magnitude of 1. Therefore, the pressure gradients in the three directions are in general of the same order of 1.

CASE I. WITH $Re = O(\frac{1}{\delta'})$

Governing Equations and Boundary Conditions

With the pressure gradient in the radial direction negligible compared to that in the circumferential and axial directions, we have the equations of motion in the latter two directions in dimensional forms,

$$\mu \frac{\partial^2 W_\varphi}{\partial r^2} = \frac{1}{r}\frac{\partial p}{\partial \varphi} \tag{15a}$$

$$\mu \frac{\partial^2 W_z}{\partial r^2} = \frac{\partial p}{\partial z} \tag{15b}$$

The simplified continuity equation in dimensional form is

$$\frac{\partial W_r}{\partial r} + \frac{1}{r}\frac{\partial W_\varphi}{\partial \varphi} + \frac{\partial W_z}{\partial z} = 0 \tag{16}$$

The boundary conditions are as follows:

(1) At the blade tip surface i.e. at $r = r_t$, (see Figs. 8 to 10).

$$W_r = W_\varphi = W_z = 0 \tag{17}$$

(2) At either casing or hub,

$$W_r = W_z = 0 \tag{18}$$

(3) At the casing for rotor blades (Figs. 8 and 10)

$$W_\varphi = -\omega r_c \tag{19}$$

At the hub for stator blades (Fig. 9)

$$W_\varphi = \omega r_h \tag{19a}$$

Variation of Velocities in the Clearance Spacing

Now, with pressure within the clearance space considered to be constant in the radial direction, the pressure p is a function of only φ and z. So are $\partial p/\partial \varphi$ and $\partial p/\partial z$. When equation (15a) is integrated twice with respect to r at a fixed set of values of φ and z, we obtain.

$$W_\varphi = \frac{1}{\mu}\frac{\partial p}{\partial \varphi}\, r(\ln r - 1) + C_1 r + C_2$$

The constants C_1 and C_2 are determined by the use of boundary conditions (17), (19) and (19a). In order to obtain one equation for either rotor blade or stator blade, we let,

$$\lambda = \frac{r_c}{r_t} \qquad \text{for rotor} \qquad (20a)$$

$$= \frac{r_h}{r_t} \qquad \text{for stator} \qquad (20b)$$

Then,

$$r_t(\ln r_t - 1)\frac{1}{\mu}\frac{\partial p}{\partial \varphi} + C_1 r_t + C_2 = 0$$

$$r_t(\ln r_t - 1)\frac{1}{\mu}\frac{\partial p}{\partial \varphi} + C_1 \lambda r_t + C_2 = \mp \omega \lambda r_t$$

where the minus sign in the last term is used for the case of rotor blades and the plus sign is used for the case of stator blades. We solve the preceding equations for C_1 and C_2 and obtain,

$$C_1 = \left(1 - \ln r_t - \frac{\lambda \ln \lambda}{\lambda - 1}\right)\frac{1}{\mu}\frac{\partial p}{\partial \varphi} \mp \frac{\lambda}{\lambda - 1}\omega$$

$$C_2 = \frac{\lambda \ln \lambda}{\lambda - 1}\frac{r_t}{\mu}\frac{\partial p}{\partial \varphi} - \left(\mp \frac{\lambda}{\lambda - 1}\omega r_t\right)$$

Hence,

$$W_\varphi = -\left[\frac{\lambda \ln \lambda}{\lambda - 1}\left(\frac{r}{r_t} - 1\right) - \frac{r}{r_t}\ln\frac{r}{r_t}\right]\frac{r_t}{\mu}\frac{\partial p}{\partial \varphi} \mp \left[\frac{\frac{r}{r_t} - 1}{\lambda - 1}\right]\lambda \omega r_t \qquad (21)$$

Similarly, integrating twice with respect to r, we obtain,

$$W_z = \frac{1}{2\mu}\frac{\partial p}{\partial z} r^2 + C_3 r + C_4$$

After the boundary conditions are used to determine the constants C_3 and C_4, we have,

$$W_z = -\left(\lambda - \frac{r}{r_t}\right)\left(\frac{r}{r_t} - 1\right)\frac{r_t^2}{2\mu}\left(\frac{\partial p}{\partial z}\right) \qquad (22)$$

Where $\lambda = \frac{r_c}{r_t} > 1$, for rotor blades and $\lambda = \frac{r_h}{r_t} < 1$ for stator blades.

Equations (21) and (22) then give the complete radial variation of the tangential and axial velocities over the clearance space. We see that the tangential velocity is composed of two parts. The first part is associated with the circumferential pressure gradient and the second part is associated with the relative motion between the blade and the wall. With the coordinate system chosen herein (see Fig. 7), the circumferential pressure gradient is a positive quantity either at the rotor blade tip (Fig. 8) of a compressor or at the stator blade tip of the turbine, and is a negative quantity either at the stator blade tip of a compressor (Fig. 9) or at the rotor blade tip of a turbine (Fig. 10). The sign of the multiplier of the pressure gradient can be seen by the use of series expansion as follows:

(1) Variation of Tangential Velocity over the Rotor Blade Tip. In this case,

$$\lambda = \frac{r_c}{r_t} = \frac{r_t + s}{r_t} = 1 + \frac{s}{r_t} \qquad (23)$$

Let $\sigma = \frac{s}{r_t}$

Then $$\lambda = 1+\sigma \tag{24}$$

$$\ln\lambda = \ln(1+\sigma) = \sigma - \frac{\sigma^2}{2} + \frac{\sigma^3}{3} - \frac{\sigma^4}{4} + \cdots \tag{25}$$

Let also $$\frac{r}{r_t} = \frac{r_t + z}{r_t} = 1 + \frac{z}{r_t} = 1 + \epsilon \tag{26}$$

Then

$$\ln\frac{r}{r_t} = \ln(1+\epsilon) = \epsilon - \frac{\epsilon^2}{2} + \frac{\epsilon^3}{3} - \frac{\epsilon^4}{4} + \cdots \tag{27}$$

and equation (21) becomes

$$W_\varphi = -\frac{\epsilon(\sigma-\epsilon)}{2}\left[1 - \frac{\sigma+\epsilon}{3} + \frac{\sigma^2+\sigma\epsilon+\epsilon^2}{6} - \cdots\right]\frac{r_t}{\mu}\frac{\partial p}{\partial\varphi} - \frac{\epsilon}{\sigma}\omega r_c$$

Let $$\eta = \frac{z}{s} = \frac{\epsilon}{\sigma} \tag{28}$$

(Note: $\eta = 0$ at $r = r_t$, $\eta = 1$ at $r = r_c$) Then,

$$W_\varphi = -\left\{\frac{\eta(1-\eta)}{2}\left[1 - \left(\frac{1+\eta}{3}\right)\sigma + \left(\frac{1+\eta+\eta^2}{6}\right)\sigma^2 - \cdots\right]\frac{s^2}{\mu r_t}\frac{\partial p}{\partial\varphi}\right.$$
$$\left. - \eta\omega r_c\right. \tag{29}$$

We see that since η and σ are numbers never greater than unity, the quantity inside the bracket is always positive. So the coefficient of $\partial p/\partial\varphi$ is always negative. The first term on the right-hand side of the equation is substantially proportional to the square of the clearance s and to the circumferential pressure gradient. It is identically equal to zero at the blade tip and at the casing wall. On the other hand, the magnitude of the second term on the right-hand side of the equation increases from zero at the blade tip to ωr_c at the casing wall.

In the case of the rotor blades in a compressor, the pressure gradient is positive and, consequently, both terms on the right-hand side are negative and their magnitudes add together.

In the case of the rotor blades in a turbine, the pressure gradient is negative, and, consequently, the two terms counteract each other.

The variation of the coefficient in the first term on the right-hand of equation (21) is plotted for several values of σ in Fig. // . It is seen that its magnitude increases at first with radius, reaches a maximum at η equals to about 0.5 and then decreases to zero at the casing.

(2) Variation of tagential velocity over the stator blade tip.

In this case,

$$\lambda = \frac{r_h}{r_t} = \frac{r_t - s}{r_t} = 1 - \frac{s}{r_t} = 1 - \sigma \tag{24a}$$

$$\ln \lambda = -\left(\sigma + \frac{\sigma^2}{2} + \frac{\sigma^3}{3} + \frac{\sigma^4}{4} + \cdots\right) \tag{25a}$$

$$\frac{r}{r_t} = \frac{r_t - \bar{s}}{r_t} = 1 - \epsilon \tag{26a}$$

$$\ln \frac{r}{r_t} = -\left(\epsilon + \frac{\epsilon^2}{2} + \frac{\epsilon^3}{3} + \frac{\epsilon^4}{4} + \cdots\right) \tag{27a}$$

and equation (21) becomes

$$W_\varphi = -\frac{\epsilon(\delta - \epsilon)}{2}\left[1 + \frac{\delta + \epsilon}{3} + \frac{\delta^2 + \delta\epsilon + \epsilon^2}{6} + \cdots\right]\frac{r_t^2}{\Lambda^2}\frac{\partial \Gamma}{\partial \varphi} + \frac{\epsilon}{\tau}(\omega r_h)$$

$$= -\frac{\eta(1-\eta)}{2}\left[1 + \frac{(1+\eta)}{3}\delta + \frac{(1+\eta+\eta^2)}{6}\delta^2 + \cdots\right]$$

We see again that the quantity inside the bracket is always a positive one and that it is always slightly greater than that in

equation (29) for the same value of σ and η . In the case of a compressor, the pressure gradient now is negative, both terms on the right-hand side of equation (30) are positive. In the case of a turbine, the pressure gradient is positive, and consequently the terms counteract each other. The first term varies with η in a similar manner as that in the rotor case. The second term varies linearly from a value of zero at r_t to a value of ωr_h at r_h .

The variation of the axial velocity as given by equation (22) can also be put in terms of the dimensionless variable η for either the rotor or the stator blade as follows:

$$W_z = -\eta(1-\eta)\frac{s^2}{2\mu}\frac{\partial p}{\partial z} \qquad (31)$$

We see that the axial velocity is proportional to s^2 and the pressure gradient and it has a parabolic variation with η inside the clearance space. Since the pressure gradient in the axial direction is always positive for compressor, the axial velocity is always negative; in the case of a turbine, the axial pressure gradient is negative and the axial velocity is positive.

Variation of Pressure in the Clearance Space

In order to compute the velocity variation by equations (21) and (22) throughout the clearance space, it is necessary to determine first the pressure gradient throughout the space. This is done as follows:

Multiplying the continuity equation by dr and integrating from the tip of a rotor blade to the casing gives,

$$\int_{r_t}^{r_c}\frac{\partial W_r}{\partial r}\,dr + \int_{r_t}^{r_c}\frac{1}{r}\frac{\partial W_\varphi}{\partial \varphi}\,dr + \int_{r_t}^{r_c}\frac{\partial W_z}{\partial z}\,dr = 0$$

But $$\int_{r_t}^{r_c} \frac{\partial W_r}{\partial r}\, dr = W_r \Big|_{r_t}^{r_c} = 0$$

Also $$\int_{r_t}^{r_c} \frac{1}{r}\frac{\partial W_\psi}{\partial \psi}\, dr = \int_{\ln r_t}^{\ln r_c} \frac{\partial W_\psi}{\partial \psi}\, d\ln r$$

Now, let

$$\alpha = \ln r$$

Then

$$\int_{r_t}^{r_c} \frac{\partial W_\psi}{\partial \psi}\, d\ln r = \int_{\alpha_t}^{\alpha_c} \frac{\partial W_\psi}{\partial \psi}\, d\alpha = \frac{\partial}{\partial \psi}\int_{\alpha_t}^{\alpha_c} W_\psi\, d\alpha + W_{\psi,r_t}\frac{\partial r_t}{\partial \psi} - W_{\psi,r_c}\frac{\partial r_c}{\partial \psi}$$

Since

$$W_{\psi,r_t} = 0, \quad \frac{\partial r_c}{\partial \psi} = \frac{\partial r_c}{\partial \psi} = 0$$

Therefore

$$\int_{r_t}^{r_c} \frac{1}{r}\frac{\partial W_\psi}{\partial \psi}\, dr = \frac{\partial}{\partial \psi}\int_{\alpha_t}^{\alpha_c} W_\psi\, d\alpha = \frac{\partial}{\partial \psi}\int_{r_t}^{r_c} \frac{W_\psi}{r}\, dr$$

Similarly,

$$\int_{r_t}^{r_c} \frac{\partial W_z}{\partial z}\, dr = \frac{\partial}{\partial z}\int_{r_t}^{r_c} W_z\, dr + W_{z,r_t}\frac{\partial r_t}{\partial z} - W_{z,r_c}\frac{\partial r_c}{\partial z}$$

Since

$$W_{z,r_c} = W_{z,r_t} = 0$$

Hence

$$\int_{r_t}^{r_c} \frac{\partial W_z}{\partial z}\, dr = \frac{\partial}{\partial z}\int_{r_t}^{r_c} W_z\, dr$$

The integral form of the continuity equation is then

$$\frac{\partial}{\partial \psi}\int_{r_t}^{r_c} \frac{W_\psi}{r}\, dr + \frac{\partial}{\partial z}\int_{r_t}^{r_c} W_z\, dr = 0 \qquad (32)$$

When the values of W_ψ and W_z as given by equations (21) and (22) are substituted into equation (32), we have,

$$\frac{\partial}{\partial \psi}\int_{r_t}^{r_c} -\left\{\left[\frac{\lambda \ln\lambda}{\lambda-1}\left(\frac{r}{r_t}-1\right) - \frac{r}{r_t}\ln\frac{r}{r_t}\right]\frac{r_t}{\mu r}\frac{\partial p}{\partial \psi} + \frac{\lambda}{\lambda-1}\left(\frac{r}{r_t}-1\right)\frac{r_t}{r}\right\} dr$$

$$+\frac{\partial}{\partial z}\int_{r_t}^{r_c} -\left\{\left(\lambda - \frac{r}{r_t}\right)\left(\frac{r}{r_t}-1\right)\frac{r_t^2}{2\mu}\frac{\partial p}{\partial z}\right\} dr = 0$$

Carrying out integration and differentiation, and rearranging, we finally obtain,

$$\left\{12\,\frac{(\lambda-1)^2-\lambda(\ln\lambda)^2}{(\lambda-1)^4}\right\}\frac{\partial^2\psi}{r_t^2\partial\varphi^2}+\frac{\partial^2\psi}{\partial z^2}=0 \qquad (33)$$

This is a linear second-order partial differential equation and can easily be transformed into a Laplace equation by letting

$$y=\left\{\frac{(\lambda-1)^4}{12\left[(\lambda-1)^2-\lambda(\ln\lambda)^2\right]}\right\}^{\frac{1}{2}} r_t\varphi \qquad (34)$$

Thus,

$$\frac{\partial^2\psi}{\partial y^2}+\frac{\partial^2\psi}{\partial z^2}=0 \qquad (35)$$

The relation between y and φ can be more clearly seen by substituting equations (23) to (27) into equation (34). This results in

$$y=\left[\frac{1}{1-\sigma+\frac{4}{10}\sigma^2+\cdots}\right] r_t\varphi$$

or

$$y=(1+\sigma+\cdots)\,r_t\varphi\approx r_c\varphi \qquad (34a)$$

Thus, y has the same sign as φ and is approximately equal to the casing radius times φ.

If the continuity equation is integrated from the stator blade tip to the hub, we again obtain equations (33) to (35). But, when the relations (23a) to (27a) are used, we obtain,

$$y = \left[\frac{1}{1+\sigma+4.1\sigma^2+\cdots}\right]\Gamma_t\varphi$$
$$= (1-\sigma-\cdots)\Gamma_t\varphi$$
$$\approx \Gamma_h\varphi \tag{34b}$$

A general approximate form for equation (34) is

$$y = \lambda\Gamma_t\varphi \tag{36}$$

and an approximate form of equation (33) is

$$\frac{1}{\lambda^2}\frac{\partial^2\phi}{\Gamma_t^2\partial\varphi^2} + \frac{\partial^2\phi}{\partial\zeta^2} = 0 \tag{37}$$

Equation (37) is a second-order partial differential equation of the elliptic type. Hence, the proper boundary condition is the pressure distribution around the blade surface at the blade tip. Like other boundary-layer problems, the potential flow outside the boundary layer has to be known in order to solve the boundary-layer flow.

The pressure distribution around the blade at the tip section is mainly determined by the geometry of the blade (the shape, the stagger angle, and the solidity), the angle of attack, the Mach number, and the Reynolds number. The influence of these factors on the tip-clearance flow is therefore exerted through the boundary condition for the solution of equation (33) or (35). As the first approximate solution, the effect of these factors on the pressure distribution around the blade tip section can be obtained either by using the theorectical calculation based on two-dimensional potential flow around the blade tip section or by using cascade tests. In the actual three-dimensional flow, the pressure distribution around the blade tip section is further influenced by the ratio of clearance to blade

height, the relative speed between the blade and the wall, the secondary boundary-layer flow across the channel formed by the blades, and the three-dimensional geometrical shape of the blade. These influences can only be determined, at the present time, by experiments, some of which are scheduled in the second phase of this research project.

With a given geometry and the pressure distribution around the blade at the tip section, equation (35) can be solved, and the circumferential and axial derivatives used in the preceding equations for the computation of the velocity components. The method of solution will be discussed after similar equations like those contained in this section are obtained for the second case.

CASE II WITH $R_e = O(1/\delta^4)$

In this case the inertia forces are in general of the same order of magnitude as the viscous force, and the pressure gradients in all three directions are of the same order of 1. In dimensional forms, the three simplified equations of motion are:

$$\frac{(W_\varphi + \omega r)^2}{r} = \frac{V^2}{r} = \frac{1}{\rho}\frac{\partial p}{\partial r} \tag{38a}$$

$$W_r \frac{\partial W_\varphi}{\partial r} + \frac{W_\varphi}{r}\frac{\partial W_\varphi}{\partial \varphi} + W_z \frac{\partial W_\varphi}{\partial z} = -\frac{1}{\rho}\frac{\partial p}{r\partial \varphi} + \nu \frac{\partial^2 W_\varphi}{\partial r^2} \tag{38b}$$

$$W_r \frac{\partial W_z}{\partial r} + \frac{W_\varphi}{r}\frac{\partial W_z}{\partial \varphi} + W_z \frac{\partial W_z}{\partial z} = -\frac{1}{\rho}\frac{\partial p}{\partial z} + \nu \frac{\partial^2 W_z}{\partial r^2} \tag{38c}$$

The simplified continuity equation is the same as in the previous case,

$$\frac{\partial W_r}{\partial r} + \frac{1}{r}\frac{\partial W_\varphi}{\partial \varphi} + \frac{\partial W_z}{\partial z} = 0 \tag{16}$$

Although the radial pressure gradient is now of the same order of magnitude of the pressure gradient in the other two directions, the total variation of pressure across the clearance space of ordinary size is still relatively small (in the order of two to three percent). (in reference 20, a measured difference of 3% across the boundary layer along the wall of a compressor is reported). Therefore, for an approximate solution, we may still ignore the radial variation of pressure for our problem, i.e. the pressure is considered to be a function of only φ and z.

Equations (38b) and (38c) each have three more inertia terms on the right-hand side of the equation than the corresponding equations of the previous case. At either the blade tip or at the bounding walls, however, these inertia terms are equal to zero, because either the

velocity component or its circumferential derivative is equal to zero. These terms exert their influence at in-between radii. Because of their presence, the equations become non-linear and it is found that an exact solution of equations (38b), (38c), and (16) cannot be obtained. In the following an approximate solution is obtained by assuming polynomial variations for the velocity components and determining the constants by the boundary conditions on the velocities and their radial derivatives as given by equations (38b) and (38c). Thus we assume

$$W_\varphi = A_0 + A_1\eta + A_2\eta^2 + A_3\eta^3 + \cdots \tag{39}$$

and

$$W_z = B_0 + B_1\eta + B_2\eta^2 + B_3\eta^3 + \cdots \tag{40}$$

The boundary conditions are as follows:

At $\eta = 0$ $(r = r_t)$,

$$W_r = 0 \tag{41a}$$

$$W_\varphi = 0 \tag{41b}$$

$$W_z = 0 \tag{41c}$$

at $\eta = 1$ ($r = r_c$ for rotor blades or $r = r_t$ for stator blades),

$$W_r = 0 \tag{41d}$$

$$W_\varphi = \mp \lambda \omega r_t \tag{41e}$$

(where the minus and positive signs are used for rotor and stator respectively)

$$W_z = 0 \tag{41f}$$

at $\eta = 0$, Equation (38b) gives

$$\frac{\partial^2 W_\psi}{\partial r^2} = \frac{1}{\mu r_t} \frac{\partial p}{\partial \psi}$$

Then,

$$\frac{\partial^2 W_\psi}{\partial \eta^2} = \frac{s^2}{\mu r_t} \frac{\partial p}{\partial \psi} \tag{41g}$$

Also, Equation (38c) gives

$$\frac{\partial^2 W_z}{\partial r^2} = \frac{1}{\mu} \frac{\partial p}{\partial z}$$

or

$$\frac{\partial^2 W_z}{\partial \eta^2} = \frac{s^2}{\mu} \frac{\partial p}{\partial z} \tag{41h}$$

At $\eta = 1$, equations (38b) and (38c) give, respectively

$$\frac{\partial^2 W_\psi}{\partial \eta^2} = \frac{s^2}{\lambda \mu r_t} \frac{\partial p}{\partial \psi} \tag{41i}$$

and

$$\frac{\partial^2 W_z}{\partial \eta^2} = \frac{s^2}{\mu} \frac{\partial p}{\partial z} \tag{41j}$$

From equations (41h) and (41j) we see that the second partial derivative of W_z with respect to η at the blade tip ($\eta = 0$) is the same as that at the wall ($\eta = 1$). In other words, the second partial derivative should not include η . Thus, equation (40) takes the form.

$$W_z = B_0 + B_1 \eta + B_2 \eta^2$$

By the use of equations (41c), (41f), and (41h), we obtain

$$B_0 = 0$$

$$B_1 = -\frac{s^2}{2\mu} \frac{\partial p}{\partial z}$$

$$B_2 = -\frac{s^2}{2\mu} \frac{\partial p}{\partial z}$$

Then

$$W_z = -\eta(1-\eta) \frac{s^2}{2\mu} \frac{\partial p}{\partial z} \tag{42}$$

On the other hand, equations (41g) and (41i) show that the

second partial derivative of W_φ with respect to η at the blade tip ($\eta = 0$) is slightly different from that at the wall ($\eta = 1$). Since we have altogether four boundary conditions for W_φ and its derivative to satisfy at the two end points, we take,

$$W_\varphi = A_0 + A_1\eta + A_2\eta^2 + A_3\eta^3 \tag{43}$$

From equations (41b), (41e), (41g), and (41j), we find

$$A_0 = 0$$
$$A_0 + A_1 + A_2 + A_3 = \mp \lambda\omega\bar{r}_t$$
$$2A_2 = \frac{s^2}{\lambda\omega\bar{r}_t}\frac{\partial p}{\partial \varphi}$$
$$2A_2 + 6A_3 = \frac{s^2}{\lambda\omega\bar{r}_t}\frac{\partial p}{\partial \varphi}$$

Solving for A_0, A_1, A_2, and A_3 and substituting them into (43) gives,

$$W_\varphi = -\left\{\frac{2\lambda+1}{6\lambda}\eta - \frac{1}{2}\eta^2 + \frac{\lambda-1}{6\lambda}\eta^3\right\}\frac{s^2}{\lambda\omega\bar{r}_t}\frac{\partial p}{\partial \varphi} \mp \lambda\omega\bar{r}_t\eta \tag{44}$$

When equations (42) and (44) obtained herein are compared to respectively, equations (31) and (21) of the previous case, we see immediately that the axial velocities as given by equations (42) and (31) are exactly the same. To compare the tangential velocities, we substitute equations (24) and (24a) into equation (44) resulting in

$$W_\varphi = -\left\{\frac{\eta(1-\eta)}{2}\left[1 - \frac{(1+\eta)}{3}\sigma - \frac{(1+\eta)}{3}\sigma^2 - \cdots\right]\right\}\left(\frac{s^2}{\lambda\omega\bar{r}_t}\frac{\partial p}{\partial \varphi}\right) - \eta\omega\bar{r}_t \tag{45}$$

for rotor blades and

$$W_\varphi = -\left\{\frac{\eta(1-\eta)}{2}\left[1 + \frac{(1+\eta)}{3}\sigma + \frac{(1+\eta)}{3}\sigma^2 + \cdots\right]\right\}\left(\frac{s^2}{\lambda\omega\bar{r}_t}\frac{\partial p}{\partial \varphi}\right) + \eta\omega\bar{r}_t \tag{46}$$

for stator blades. In these forms, we see that equations (45) and (46) are also equal to the corresponding equations (29) and (30) of the previous case if terms involving σ^2 and higher orders are neglected.

This is usually permissible, since ϵ is a very small quantity.

Hence we see that if the radial variations of the velocity components in this case can be represented by polynomials, the equations for the velocities are the same as those of the previous case. The validity of the assumption of polynomial representation in this case should be verified in the future experiments. It should be noted that, although the equations are the same, the pressure distribution around the tip blade section and, consequently, the circumferential and axial gradients of pressure can be a function of Reynolds number. Therefore, the actual velocities can still be a function of Reynolds number. The values of μ in the two cases are also different.

Inasmuch as the velocities of this case are the same as those in the previous case, equations (34), (35), (36), and (37) obtained in the previous case can also be used for this case.

SOLUTION OF PRESSURE DISTRIBUTION IN CLEARANCE SPACE

From the preceding two sections we see that the pressure distribution across the clearance space is to be determined by the equation

$$\frac{1}{(\lambda r_t)^2}\frac{\partial^2 P}{\partial \varphi^2} + \frac{\partial^2 P}{\partial z^2} = 0 \qquad (37)$$

or

$$\frac{\partial^2 P}{\partial y^2} + \frac{\partial^2 P}{\partial z^2} = 0 \qquad (35)$$

where

$$y = \lambda r_t \varphi \qquad (36)$$

$$= r_c \varphi \quad \text{for rotor blades} \qquad (34a)$$

$$= r_h \varphi \quad \text{for stator blade} \qquad (34b)$$

Now, the difficulty in solving the pressure distribution lies in the arbitrary boundary values of the pressure given around the blade section of agiven arbitrary shape. In general, a sufficiently accurate answer can be obtained by the use of relaxation or matrix method (Reference 20, 21). The difficulty introduced by the non-uniform grid spacings can be helped out by the use of differentiation formulas for non-uniform spacings (Reference 20. See example on pp. 27-29 for the use of these formulas in conjunction with either the relaxation or matrix method).

A second method of solution is to replace the given blade section by a Joukowsky airfoil section and to solve for the pressure variation over the airfoil section after a conformal transformation which converts the airfoil into a circle. This method of solution is given below.

Approximation of the Given Tip Section by a Joukowsky Airfoil

Figure 13 shows the blade tip section in the y - z plane. χ is the angle between z-axis and the chord line which connects the leading edge and the trailing edge of the airfoil. Also shown is the Joukowsky airfoil approximating this tip section. This Joukowsky airfoil is obtained by matching the chord, the thickness ratio and the camber (maximum value of mean line ordinate).

Referring to Figure 13, we first make a transformation of coordinates from y - z to y' - z' by,

$$\left.\begin{aligned} y' &= -y\cos\chi - z\sin\chi \\ -z' &= z\cos\chi - y\sin\chi \end{aligned}\right\} \tag{47}$$

Then this Joukowsky airfoil with its chord (C) lying on the z'-axis is obtained by transforming a circle of radius 'a' with center at M in the ζ-η plane by the Joukowsky transformation :

$$x = \zeta + \frac{c^2}{\zeta} \tag{48}$$

where

$$\zeta = \xi + i\eta \tag{49}$$

$$x = z' + iy' \tag{50}$$

$$C = 4c(1+m^2) \tag{51}$$

$$a = c(1+m) \tag{52}$$

(m is a small quantity)

The coordinates of the airfoil are given by

$$\left.\begin{aligned} x' &= \left(b + \frac{c^2}{b}\right)\cos\theta \approx 2c\cos\theta \\ y' &= \left(b - \frac{c^2}{b}\right)\sin\theta \approx 2c\sin\theta\left[m(1+\cos\theta) + \beta\sin\theta\right] \end{aligned}\right\} \quad (53)$$

where

$$\beta = \tan^{-1}\frac{m\cos\delta}{c + m\sin\delta} \approx \frac{m\cos\delta}{c + m\sin\delta} \qquad (54)$$

and is a small angle.

From eqs. (53), the maximum thickness is equal to $3\sqrt{3}/4\ mc$ which occurs at one-quarter of the chord from the leading edge and the camber is equal to $1/2\ \beta$. In the approximation of the given blade tip section by the Joukowsky airfoil, the geometrical data of the tip section is to be used to obtain C (or c), m, and β of the Joukowsky airfoil.

Velocity and Pressure Distributions Around the Joukowsky Airfoil

In the ζ-plane, the velocity at the surface of the circle is

$$W_\zeta = 2W_0\sin(\alpha + \psi) + \frac{\Gamma}{2\pi a}$$

But

$$\Gamma = 4\pi a W_0 \sin(\alpha + \beta)$$

Hence

$$W_\zeta = 2W_0\left[\sin(\alpha+\psi) + \sin(\alpha+\beta)\right] \qquad (55)$$

The velocity around the airfoil in the z-plane and that around the circle in the ζ-plane are related by

$$|W_z| = \frac{|W_\zeta|}{\left|\frac{dz}{d\zeta}\right|} \qquad (56)$$

where $$\left|\frac{dx}{d\zeta}\right| = \left|1 - \frac{c^2}{\zeta^2}\right| = \left|\sqrt{\left(1 - \frac{c^2}{b^2}\cos 2\theta\right)^2 + \left(\frac{c^2}{b^2}\sin 2\theta\right)^2}\right|$$

$$= \left|\sqrt{\left(1 - \frac{c^2}{b^2}\right)^2 + 4\left(\frac{c}{b}\right)^2 \sin^2\theta}\right| \qquad (57)$$

From Fig. 13, we see

$$b\sin\theta = a(\sin\psi + \sin\beta)$$
$$b\cos\theta = a\cos\psi + lc \qquad (58)$$

and

$$a\cos\beta = c(1+l) \qquad (59)$$

Hence

$$\left(\frac{c}{b}\right)^2 = \frac{1}{(1+l)^2\sec^2\beta(\sin\psi+\sin\beta)^2 + \left[(1+l)\sec\beta\cos\psi + l\right]^2} \qquad (60)$$

Substituting equations (55), (57) and (60) into equation (56) gives

$$\left(\frac{W_x}{W_0}\right)^2 = \frac{\sec^2\beta\left[1-\cos(2\alpha+\psi+\beta)\right]\left\{\left[1+\sin^2\beta+2\sin\beta\sin\psi\right] + 4l\cos\left(\frac{\psi-\beta}{2}\right)\left[\sin\beta\sin\left(\frac{\psi+\beta}{2}\right)+(1+l)\cos\left(\frac{\psi-\beta}{2}\right)\right]\right\}^2}{2\left\{\tan\beta\sin\left(\frac{\psi+\beta}{2}\right)+l\sec\beta\left[\sin\beta\sin\left(\frac{\psi-\beta}{2}\right)+(1+l)\cos\left(\frac{\psi-\beta}{2}\right)\right]\right\}^2 + (1+l)^2\left[1-\cos(\psi+\beta)\right]} \qquad (61)$$

Equation (61) now gives the velocity distribution around the airfoil in terms of W_0, α, β, l and ψ. For a given airfoil and a given approach velocity at a given angle of attack, β, l, W_0 and α are fixed values.

The pressure distribution around the airfoil is obtained by the use of Bernoulli equation and the velocity distribution given by Equation (61)

$$p = p_0 + \frac{1}{2}\rho_0 W_0^2\left\{1 - \frac{\sec^2\beta\left[1-\cos(2\alpha+\psi+\beta)\right]\left\{\left[1+\sin^2\beta+2\sin\beta\sin\psi\right] + 4l\cos\left(\frac{\psi-\beta}{2}\right)\left[\quad\right]\right\}^2}{2\left\{\tan\beta\sin\left(\frac{\psi+\beta}{2}\right)+l\sec\beta\left[\quad\right]\right\}^2 + (1+l)^2\left[1-\cos(\psi+\beta)\right]}\right\} \qquad (62)$$

Solution of the Laplace Equation in Pressure

With the boundary values of the pressure around the airfoil section given by equation (62), the variation of pressure across the blade tip is obtained by the solution of equation (35). Because of the complicated boundary shape of the airfoil in the z'-y' plane, we attempt to solve the equation in conformall-transformed ζ-plane with the simple circular boundary. To do this, the Laplace equation is expressed in polar coordinates R and ψ (Fig. 14).

$$\frac{\partial^2 p}{\partial R^2} + \frac{1}{R}\frac{\partial P}{\partial R} + \frac{1}{R^2}\frac{\partial^2 P}{\partial \psi^2} = 0 \tag{63}$$

The solution of this equation can be expressed in a Fourier series as follows (see reference 22):-

$$p(R,\psi) = A_0 + \sum_{n=1}^{\infty}\left(\frac{R}{a}\right)^n (A_n \cos n\psi + B_n \sin n\psi) \tag{64}$$

In order to determine the Fourier coefficients A's and B's, we first write equation (64) at the boundary R = a:

$$p(a,\psi) = A_0 + \sum_{n=1}^{\infty}(A_n \cos n\psi + B_n \sin n\psi) \tag{65}$$

Then we express the known boundary values, equation (62) in a Fourier series:

$$p(a,\psi) = A_0' + \sum_{n=1}^{\infty}(A_n' \cos n\psi + B_n' \sin n\psi) \tag{66}$$

Equating equations (65) and (66) gives

$$\left.\begin{aligned} A_0 &= A_0' \\ A_n &= A_n' \\ B_n &= B_n' \end{aligned}\right\} \tag{67}$$

In the case of cambered Joukowsky airfoil, it is quite a complicated process to express explicitly the $A's$ and $B's$ in terms of W_0, α, β and ℓ.

In case it is desirable to solve the present problem with an experimentally measured pressure distribution around the tip blade section, one can obtain the coefficients $A_n's$ and $B_n's$ by a suitable numerical method and then obtain $A_n's$ and $B_n's$ by equations (67).

In the case of a symmetrical Joukowsky section, it is found relatively simple to obtain a general expression for the coefficients (based on the theoretical pressure distribution. In this special case,

$$\beta = 0$$

and

$$\left(\frac{W_x}{W_0}\right)^2 = \frac{\left\{1+4(1+\cos\psi)\ell\left[1+(2+\cos\psi)\ell\right]\right\}\left[1-\cos 2\alpha\cos\psi+\sin 2\alpha\sin\psi\right]}{\left[(1-\cos\psi)+2(1-\cos\psi)\ell+2\ell^2\right]} \qquad (68)$$

Based on this equation we found, by the method given in reference 23 and using 30° intervals,

$$A_0 = p_0 + \tfrac{1}{2}\rho_0 W_0^2\left\{1-\left[\left(\frac{1}{24\ell^2}+\frac{1}{3\ell}+2.99+8.43\ell\right)-\left(\frac{1}{24\ell^2}+\frac{1}{3\ell}+2.07+6.75\ell\right)\cos 2\alpha\right]\right\}$$

$$A_1 = -\left(\tfrac{1}{2}\rho_0 W_0^2\right)\left\{\left(\frac{1}{12\ell^2}+\frac{1}{1.5\ell}+4.14+13.5\ell\right)-\left(\frac{1}{12\ell^2}+\frac{1}{1.5\ell}+4.30+10.88\ell\right)\cos 2\alpha\right\}$$

$$A_2 = -\left(\tfrac{1}{2}\rho_0 W_0^2\right)\left\{\left(\frac{1}{12\ell^2}+\frac{1}{1.5\ell}+2.64+4.5\ell\right)-\left(\frac{1}{12\ell^2}+\frac{1}{1.5\ell}+2.80+5.5\ell\right)\cos 2\alpha\right\}$$

$$A_3 = -\left(\tfrac{1}{2}\rho_0 W_0^2\right)\left\{\left(\frac{1}{12\ell^2}+\frac{1}{1.5\ell}+1.47-2.5\ell\right)-\left(\frac{1}{12\ell^2}+\frac{1}{1.5\ell}+1.64-1.5\ell\right)\cos 2\alpha\right\}$$

$$A_4 = -\left(\tfrac{1}{2}\rho_0 W_0^2\right)\left\{\left(\frac{1}{12\ell^2}+\frac{1}{1.5\ell}+.64-7.5\ell\right)-\left(\frac{1}{12\ell^2}+\frac{1}{1.5\ell}+0.81-6.5\ell\right)\cos 2\alpha\right\}$$

$$A_5 = -\left(\tfrac{1}{2}\rho_0 W_0^2\right)\left\{\left(\frac{1}{12\ell^2}+\frac{1}{1.5\ell}+.14-10.5\ell\right)-\left(\frac{1}{12\ell^2}+\frac{1}{1.5\ell}+.31-9.5\ell\right)\cos 2\alpha\right\}$$

$$A_6 = -\left(\tfrac{1}{2}\rho_0 W_0^2\right)\left\{\left(\frac{1}{24\ell^2}+\frac{1}{3\ell}-5.74\ell\right)-\left(\frac{1}{24\ell^2}+\frac{1}{3\ell}+.07-5.25\ell\right)\cos 2\alpha\right\}$$

$$B_1 = -\left(\tfrac{1}{2}\rho_0 W_0^2\right)\left\{(1.67+6\ell)\sin 2\alpha\right\}$$

$$B_2 = -\left(\tfrac{1}{2}\rho_0 W_0^2\right)\left\{(1.33+8\ell)\sin 2\alpha\right\} \qquad (69)$$

$$B_3 = -\left(\tfrac{1}{2}\rho_0 W_0^2\right)\left\{(1+6\ell)\sin 2\alpha\right\}$$

$$B_4 = -\left(\tfrac{1}{2}\rho_0 W_0^2\right)\left\{(.67+4\ell)\sin 2\alpha\right\},\quad B_5 = -\left(\tfrac{1}{2}\rho_0 W_0^2\right)\left\{(.33+2\ell)\sin 2\alpha\right\}$$

These expressions are general that it can be used for any values of ℓ and α .

Pressure Gradient

To obtain the pressure gradient, we differentiate equation (64) with respect to R and ψ , respectively

$$\left.\begin{aligned}\frac{\partial p}{\partial R} &= \sum_{n=1}^{\infty}\left(n A_n R^{n-1}\cos n\psi + n B_n R^{n-1}\sin n\psi\right)\\ \frac{\partial p}{\partial \psi} &= \sum_{n=1}^{\infty}\left(-n A_n R^{n}\sin n\psi + n B_n R^{n}\cos n\psi\right)\end{aligned}\right\} \qquad (70)$$

To lead these derivatives to $\frac{\partial p}{\partial \phi}$ and $\frac{\partial p}{\partial z}$, we have to find the relations among $\frac{\partial p}{\partial R}$, $\frac{\partial p}{\partial \psi}$, $\frac{\partial p}{\partial y'}$, $\frac{\partial p}{\partial z'}$, $\frac{\partial p}{\partial y}$ and $\frac{\partial p}{\partial z}$. From equations(53),(54),(55) and referring to Figure 13, we obtain,

$$\left.\begin{aligned}z' &= \left(R' + \frac{c^2}{R'^2}\right)\cos\theta = R'\cos\theta\left(1+\frac{c^2}{R'^2}\right)\\ y' &= \left(R' - \frac{c^2}{R'^2}\right)\sin\theta = R'\sin\theta\left(1-\frac{c^2}{R'^2}\right)\end{aligned}\right\} \qquad (71)$$

$$\left.\begin{aligned}R'\sin\theta &= R\sin\psi + a\sin\beta\\ R'\cos\theta &= R\cos\psi + \ell c\end{aligned}\right\} \qquad (72)$$

Equations (71) and (72) give,

$$z' = (R\cos\psi + \ell c)\left\{1 + \frac{c^2}{\left[(1+\ell)^2 c^2\tan^2\beta + \ell^2 c^2\right] + 2\ell c R\cos\psi + 2(1+\ell)cR\tan\beta\sin\psi + R^2}\right\}$$

$$y' = \left[R\sin\psi + (1+\ell)c\tan\beta\right]\left\{1 - \frac{c^2}{\left[(1+\ell)^2 c^2\tan^2\beta + \ell^2 c^2\right] + 2\ell c R\cos\psi + 2(1+\ell)cR\tan\beta\sin\psi + R^2}\right\}$$

Differentiating the preceding equations with respect to z' gives,

$$1 = \left\{ -\frac{2(1+\ell)\ell c^4 \tan\beta \sin\psi}{D^2} - \frac{2(1+\ell)c^3 R \tan\beta \sin\psi\cos\psi}{D^2} + \left(1 + \frac{c^2}{D} - \frac{2\ell c^2 \psi}{D^2} - \frac{2c^2R^2}{D^2}\right)\cos\psi - \frac{2\ell c^3 R}{D^2}\cos^2\psi - \frac{2\ell c^3 R}{D^2}\right\}\frac{\partial R}{\partial z'} + \left\{ -\left(R + \frac{c^2 R}{D} - \frac{2\ell^2 c^4 R}{D^2}\right)\sin\psi + \frac{2\ell c^3 R^2}{D^2}\sin\psi\cos\psi - \frac{2(1+\ell)\ell c^4 R\tan\beta}{D^2}\cos\psi - \frac{2(1+\ell)c^3\tan\beta R^2}{D^2}\cos^2\psi\right\}\frac{\partial\psi}{\partial z'}$$

$$0 = \left\{ \frac{2(1+\ell)c^3 R\tan\beta}{D^2}\sin^2\psi + \left(1 - \frac{c^2}{D} + \frac{2c^2R^2}{D^2} + \frac{2(1+\ell)^2 c^4\tan^2\beta}{D^2}\right)\sin\psi + \frac{2\ell c^3 R}{D^2}\sin\psi\cos\psi + \frac{2(1+\ell)\ell c^4\tan\beta}{D^2}\cos\psi + \frac{2(1+\ell)c^3 R\tan\beta}{D^2}\right\}\frac{\partial R}{\partial z'} + \left\{ -\frac{2\ell c^3 R^2}{D^2}\sin^2\psi - \frac{2(1+\ell)\ell c^4 R\tan\beta}{D^2}\sin\psi + \frac{2(1+\ell)c^3 R^2\tan\beta}{D^2}\sin\psi\cos\psi + \left[R - \frac{c^2 R}{D} + \frac{2(1+\ell)^2 c^4 R\tan\beta}{D^2}\right]\cos\psi\right\}\frac{\partial\psi}{\partial z'}$$

where $D = (R^2 + c^2\tan^2\beta + 2cR\tan\beta\sin\psi) + 2c)(R\cos\psi + R\tan\beta\sin\psi + c\tan^2\beta)\ell + c^2\sec^2\beta\,\ell^2$

By sol ing for $\frac{\partial R}{\partial z'}$ and $\frac{\partial\psi}{\partial z'}$ we obtain

$$\frac{\partial R}{\partial z'} = \frac{\left\{(1+\ell)cR\tan\beta\sin 2\psi + \ell cR\cos 2\psi - 2(1+\ell)\ell c^2\tan\beta\sin\psi + \left[\frac{D^2}{c^2} - D + 2(1+\ell)^2 c^2\tan^2\beta\right]\cos\psi - \ell cR\right\}(D)}{M}$$

$$\frac{\partial\psi}{\partial z'} = \frac{-\left\{\ell cR\sin 2\psi - (1+\ell)cR\tan\beta\cos 2\psi + \left[\frac{D^2}{c^2} - D + 2R^2 + 2(1+\ell)^2 c^2\tan^2\beta\right]\sin\psi + \left[2(1+\ell)\ell c^2\tan\beta\right]\cos\psi + 3(1+\ell)cR\tan\beta\right\}(D)}{RM} \qquad (73)$$

Where $$M = \Big\{ 4(1+\ell)cR\tan\beta(D+c^2)\sin\psi - 4\ell cR(D-c^2)\cos\psi - 2R^2D\cos 2\psi + \Big\{ \frac{D^3}{c^2} - c^2D - 2(D-c^2)\ell^2c^2 + 2(D+c^2)(1+\ell)^2c^2\tan^2\beta + 2c^2R^2 \Big] \Big\}$$

Similarly, differentiating with respect to y' leads to

$$\frac{\partial R}{\partial y'} = -\frac{\Big\{ \ell cR\sin 2\psi - (1+\ell)cR\tan\beta\cos 2\psi - \big(\frac{D^2}{c^2} + D - 2\ell^2c^2\big)\sin\psi - 2(1+\ell)\ell c^2\tan\beta\cos\psi - (1+\ell)cR\tan\beta \Big\}(D)}{M} \tag{74}$$

$$\frac{\partial \psi}{\partial y'} = -\frac{\Big\{ (1+\ell)cR\tan\beta\sin 2\psi + \ell cR\cos 2\psi + 2\ell(1+\ell)c^2\sec\beta\sin\psi - \big(\frac{D^2}{c^2} + D - 2\ell^2c^2 - 2R^2\big)\cos\psi + 3\ell cR \Big\}(D)}{RM}$$

In particular at $R = a = (1+\ell)c\sec\beta$, equations (73) and (74) reduce to,

$$\Big(\frac{\partial R}{\partial y'}\Big)_a = \frac{\Big\{ (1+\ell)^2\tan\beta\sec\beta\sin 2\psi + \ell(1+\ell)\sec\beta\cos 2\psi - 2\ell(1+\ell)\tan\beta\sin\psi + \Big[\frac{D_a^2}{c^4} - \frac{D_a}{c^2} + 2(1+\ell)^2\tan^2\beta \Big]\cos\psi - (1+\ell)\ell\sec\beta \Big\}(D_a)}{Ma}$$

$$\Big(\frac{\partial \psi}{\partial y'}\Big)_a = -\frac{\Big\{ \ell(1+\ell)\sec\beta\sin 2\psi - (1+\ell)^2\sec\beta\cos 2\psi + \Big[\frac{D_a^2}{c^4} - \frac{D_a}{c^2} + 2(1+\ell)^2\sec^2\beta + 2(1+\ell)^2\tan^2\beta \Big]\sin\psi + 2\ell(1+\ell)\tan\beta\cos\psi + 3(1+\ell)^2\tan\beta\sec\beta \Big\}(D_a)}{(1+\ell)c\sec\beta\, Ma}$$

$$\Big(\frac{\partial R}{\partial y'}\Big)_a = -\frac{\Big\{ \ell(1+\ell)\sec\beta\sin 2\psi - (1+\ell)^2\tan\beta\sec\beta\cos 2\psi - \Big[\frac{D_a^2}{c^4} + \frac{D_a}{c^2} - 2\ell^2 \Big]\sin\psi - 2\ell(1+\ell)\tan\beta\cos\psi - (1+\ell)^2\tan\beta\sec\beta \Big\}(D_a)}{Ma} \tag{75}$$

$$\Big(\frac{\partial \psi}{\partial y'}\Big)_a = -\frac{\Big\{ (1+\ell)^2\tan\beta\sec\beta\sin 2\psi + \ell(1+\ell)\sec\beta\cos 2\psi + 2\ell(1+\ell)\sec\beta\sin\psi - \Big[\frac{D_a^2}{c^4} + \frac{D_a}{c^2} - 2\ell^2 - 2(1+\ell)^2\sec^2\beta \Big]\cos\psi + 3\ell(1+\ell)\sec\beta \Big\}(D_a)}{(1+\ell)c\sec\beta\, Ma}$$

Where,

$$M_a = \Big\{ 4(1+\ell)^2 (D_a + C^2) \tan\beta \sec\beta \sin\psi - 4\ell(1+\ell)(D_a - C^2) \sec\beta \cos\psi$$
$$- 2(1+\ell)^2 D_a \sec^2\beta \cos 2\psi + \Big\{ \frac{E_i^3}{C^4} - D_a - 2(D_a - C^2)\ell^2$$
$$+ 2(D_a + C^2)(1+\ell)^2 \tan^2\beta + 2(1+\ell)^2 C^2 \sec^2\beta \Big\}$$

$$D_a = C^2 \sec^2\beta \Big\{ (1 + \sin^2\beta + 2\sin\beta\sin\psi) + 2(1 + \sin^2\beta$$
$$+ 2\sin\beta\sin\psi + \cos\beta\cos\psi)\ell + 2(1 + \sin\beta\sin\psi$$
$$+ \cos\beta\cos\psi)\ell^2 \Big\}$$

Having found these derivatives, we can compute $\left(\frac{\partial p}{\partial z'}\right)_a$ and $\left(\frac{\partial p}{\partial y'}\right)_a$ by

$$\left(\frac{\partial p}{\partial z'}\right)_a = \left(\frac{\partial p}{\partial R}\right)_a \left(\frac{\partial R}{\partial z'}\right)_a + \left(\frac{\partial p}{\partial \psi}\right)_a \left(\frac{\partial \psi}{\partial z'}\right)_a$$
$$\left(\frac{\partial p}{\partial y'}\right)_a = \left(\frac{\partial p}{\partial R}\right)_a \left(\frac{\partial R}{\partial y'}\right)_a + \left(\frac{\partial p}{\partial \psi}\right)_a \left(\frac{\partial \psi}{\partial y'}\right)_a \qquad (76)$$

Where $\left(\frac{\partial p}{\partial R}\right)_a$ and $\left(\frac{\partial p}{\partial \psi}\right)_a$ can be obtained from equation (70) by putting R = a,

$$\left.\begin{aligned} \left(\frac{\partial p}{\partial R}\right)_a &= \sum_{n=1} \left(n A_n a^{n-1} \cos n\psi + n B_n a^{n-1} \sin n\psi\right) \\ \left(\frac{\partial p}{\partial \psi}\right)_a &= \sum_{n=1} \left(-n A_n a^n \sin n\psi + n B_n a^n \cos n\psi\right) \end{aligned}\right\} \qquad (77)$$

From equations (47),

$$\frac{\partial y'}{\partial y} = -\cos\chi, \qquad \frac{\partial y'}{\partial z} = -\sin\chi$$
$$\frac{\partial z'}{\partial z} = -\cos\chi, \qquad \frac{\partial z'}{\partial y} = +\sin\chi$$

Therefore,

$$\left.\begin{aligned} \left(\frac{\partial p}{\partial y}\right)_a &= -\cos\chi \left(\frac{\partial p}{\partial y'}\right)_a + \sin\chi \left(\frac{\partial p}{\partial z'}\right)_a \\ \left(\frac{\partial p}{\partial z}\right)_a &= -\sin\chi \left(\frac{\partial p}{\partial y'}\right)_a - \cos\chi \left(\frac{\partial p}{\partial z'}\right)_a \end{aligned}\right\} \qquad (78)$$

From Equation (36)

$$\left(\frac{\partial p}{\partial \eta}\right)_a = \lambda \tau \left(\frac{\partial p}{\partial y}\right)_a \tag{79}$$

Equations (70), (73), (74), (76), (77) and (78) altogether give $\left(\frac{\partial p}{\partial \eta}\right)_a$ and $\left(\frac{\partial p}{\partial z}\right)_a$, which are required to compute the velocity distribution across the tip clearance space as given by equations (42) and (45) or (46).

Alternate Approximation

Instead of approximating the given tip blade section by a Joukowsky section, as stated on p. 36, one may transform the given blade section by the Joukowsky transformation into a near circle, which can then be approximate by a true circle, thereby determining the values of m and β . The rest of the procedure remains the same.

MASS FLOW ACROSS TIP-CLEARANCE SPACE

After the velocity distribution across the tip-clearance space is obtained, the mass flow across it can be obtained by adding together the mass flow in the tangential and in the axial directions. In the tangential direction, the mass flow is (Figure 15).

$$Q_\varphi = \rho \int_0^{C\cos\chi} \int_{r_t}^{r_c} W_\varphi \, dr \, dz$$

In the axial direction, the mass flow is,

$$Q_z = \rho \int_0^{C\sin\chi} \int_{r_t}^{r_c} W_z \, dr \, dy$$

Therefore, the resultant mass flow across the tip-clearance space will be, (Figure 15)

$$\begin{aligned} Q &= - Q_\varphi - Q_z \\ &= - \rho \left\{ \int_0^{C\cos\chi} \int_{r_t}^{r_c} W_\varphi \, dr \, dz - \int_0^{C\sin\chi} \int_{r_t}^{r_c} W_\varphi \, dr \, dy \right\} \end{aligned} \tag{80}$$

SUMMARY

A basic analysis is made on the flow phenomena across the blade tip clearance space. The fluid is considered to be viscous and incompressible and the basic equations of motion and continuity are expressed with respect to a cylindrical coordinate system rotating with the blades at the same speed.

Simplified equations are then obtained by an order-of-magnitude analysis. Two cases are considered; one with low Reynolds number and one with high Reynolds number.

In the first case, the equations of motion can be solved to give an analytical expression for the velocity distributions in the clearance space in terms of the pressure gradient and the relative speed between the blade and the bounding wall. The pressure distribution is governed by a Laplace equation which is obtained from the continuity equation.

In the second case, the equations of motion cannot be solved analytically. An approximate solution is obtained by assuming a third order polynomial for the tangential velocity and a second order polynomial for the axial velocity and using the proper boundary conditions. The form of the equations obtained is very similar to that of the first case.

Three methods of solution are discussed for the solution of the Laplace equation of pressure distribution. One is a direct numerical solution by either the relaxation method or matrix method. The next one involves an approximation of the tip section by a Joukowsky section. The last one involves a transformation of the given blade section by

the Joukowsky transformation into a near circle, which is then approximated by a true circle. In either of the last two methods the pressure distribution in the transformed plane is expressed in the form of a Fourier series. Either the theoretical or experimentally obtained pressure distribution along the blade surface can be used as the boundary values. Expressions are obtained to convert the pressure gradients obtained in the transformed plane to those in the actual blade tip section.

Finally an expression for the mass flow across the tip clearance space is obtained.

The pressure gradient over the blade section at the blade tip is found to be affected by factors such as blade loading (i.e. pressure distribution over blade section) shape of blade airfoil section, casing wall boundary layer, viscosity of the fluid, relative motion between the casing wall and the blade tip. Velocities through the tip-clearance is found to be primarily determined by the pressure gradient and varies with the square of the tip-clearance, while mass flow across the tip-clearance is found to be determined by the velocity distribution, hence by the pressure gradient and varies with the cube of the tip-clearance.

REFERENCES

1. Wu, Chung-Hua: Survey of Available Information on Internal Flow losses through Axial Turbomachines. NACA RME50J13, Jun. 26, 1951.

2. Brunot, A. & Fulton, R.: A clearanceometer for Determining Blade-tip clearances of Axial-Flow Compressors - Trans. ASME, Jan. 1953.

3. Carter, A.: 3-D'al Flow Theories for Axial Compressors and Turbines - Internal Combustion Turbines.

4. Echert, B.: Summary of the results of Research on Axial Flow Compressors - BUSHIPS 338, Navy Dept., May 1946.

5. Ainley & Jeffs: Analysis of the Air Flow Through 4-Stages of Half-Vortex Blading in an Axial Compressor - British ARC RM 2383, Apr. 1946.

6. Speakman, E.: The Determination of Principal Dimensions of the Steam-Turbine - Trans. of the Institution of Engrs. & Shipbuilders in Scotland. Vol. 49.

7. Betz, A.: The phenomena at the Tips of Kaplan Turbines - Hydraulische Probleme, June, 1925.

8. Sedille, M.: Mechanics of Fluids on Axial Compressors and the Influence of Clearance - Comptes Rendus, May & June 1939.

9. Meldahl, A.: The End Loss of Turbine Blades - The Brown Boveri Rev. Nov. 1941.

10. Traupel, W.: New General Theory of Multistage Axial Flow Turbomachines, Navships 250-445-1, Navy Dept. 1942.

11. Fickert: The Influence of the Radial Clearance of the Rotor on the Compressor Efficiency - Buships 338, Navy Dept. May 1946.

12. Ruden, P.: Investigation of Single Stage Axial Fans NACA RM 1062.

13. Lindsey, W.: The Development of the Armstrong Siddeley Mamba Engine-Roy. Aero. Soc. J. 1949.

14. Schaffer, H.: Messungen der Spaltverluste eines ebenen Schaufelgitters - Rep. No. 52/17 of the Institute of Fluid Mechanics of the Technical Univ. of Braunschweig.

15. Hansen, A, Herzig, H., Costello, G.: A visualization study of Secondary Flows In Cascades NACA TN 2947.

16. Guinard, Fuller and Acosta: An Experimental Study of Axial Flow Pump Cavitation - Hydrodynamic Lab. CIT Rep. No. E-193-Aug. 1953.

17. Carter, A. & Cohen, E.: Preliminary Investigation into the

3-Dimensional Flow Through a Cascade of Aerofoils - British ARC RM 2339-1949.

18. Squire, H.B. & Winter, K.G.: The Secondary Flow in a Cascade of Airfoils in a Nonuniform Stream - J. of Aero. Sci. Vol. 18, No. 4 Apr. 1951.

19. Wu, C.H. and Wolfenstein, L.: Application of Radial Equilibrium to Axial-Flow Compressor and Turbine Design - NACA TR 955-1950.

20. Southwell, R.V.: Relaxation Methods in Theoretical Physics. Clarendon Press (Oxford), 1946.

21. Wu, C. H.: Formulas and Tables of Coefficients for Numerical Differentiation with Function Values Given at Unequally Spaced Points and Application to Solution of Partial Differential Equations, NACA T.N. 2214, Nov. 1950.

22. Hildbrand, F. B.: Advanced Calculus for Engineers pp. 423 - 426.

23. Scarborough, J. B.: Numerical Mathematical Analysis Chapter XVII.

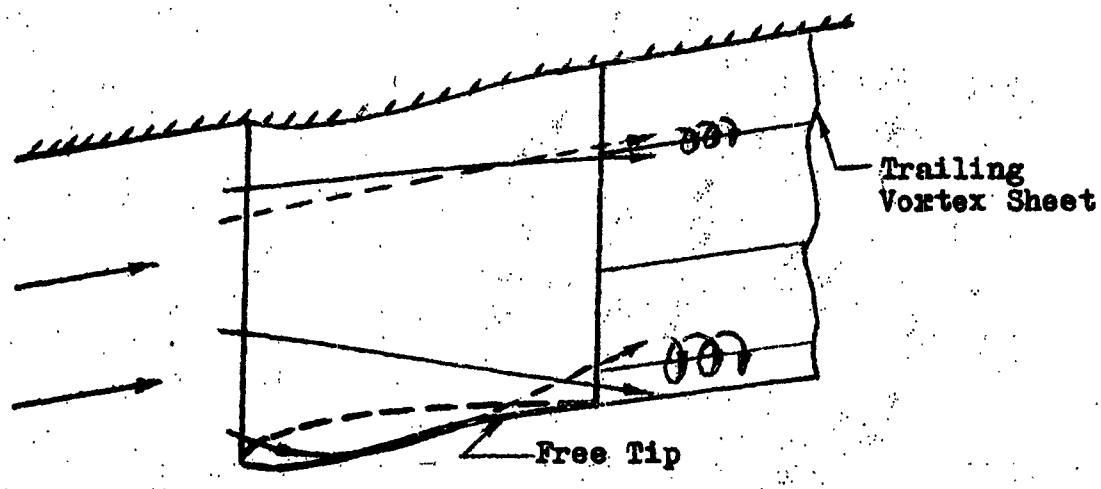

FIG. 1 - Flow Past Free Tip Blade.

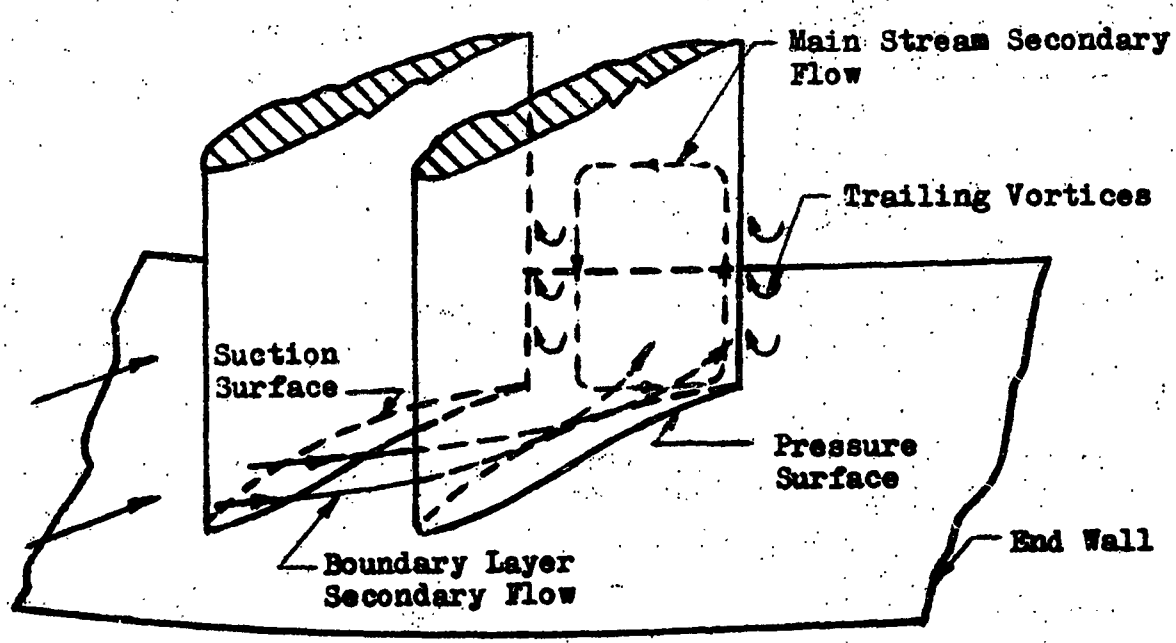

FIG. 2 - Flow Past Blades With End- Wall.

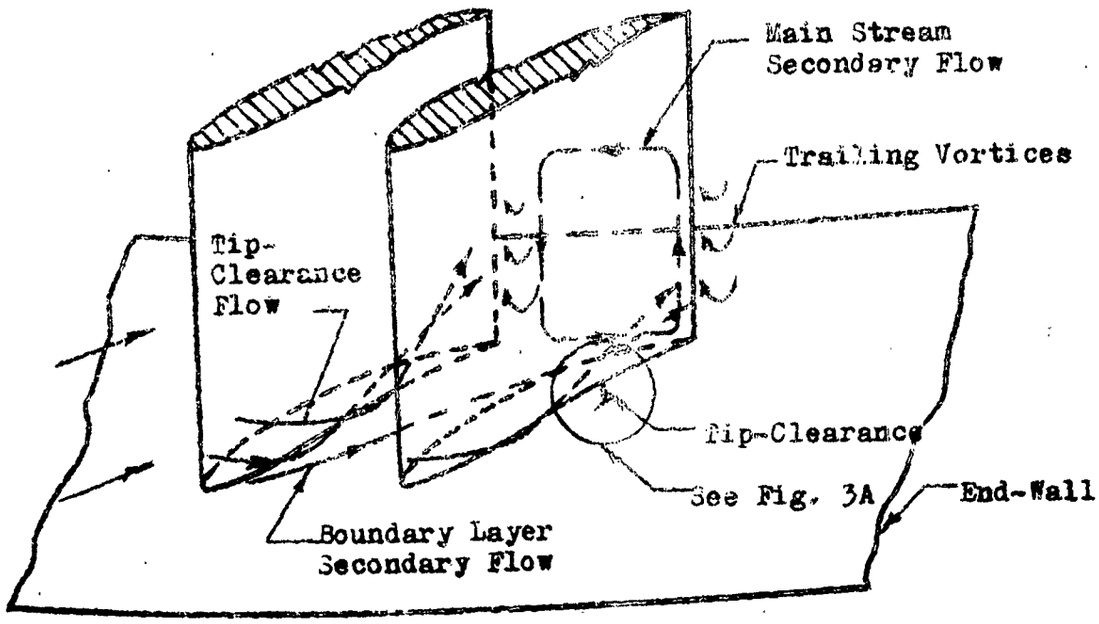

FIG. 3 - Flow Past Blades With Stationary End-Wall And Tip-Clearance.

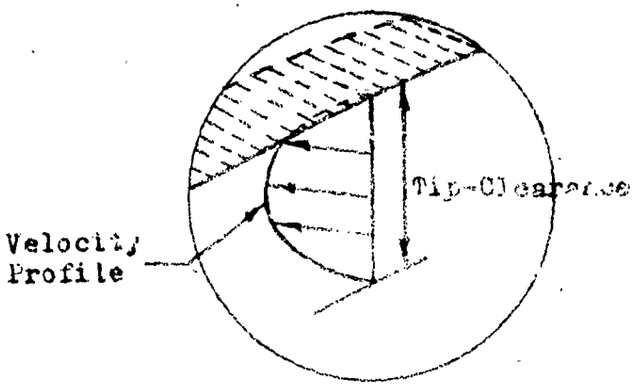

FIG. 3A - Details of Flow Inside Clearance Space.

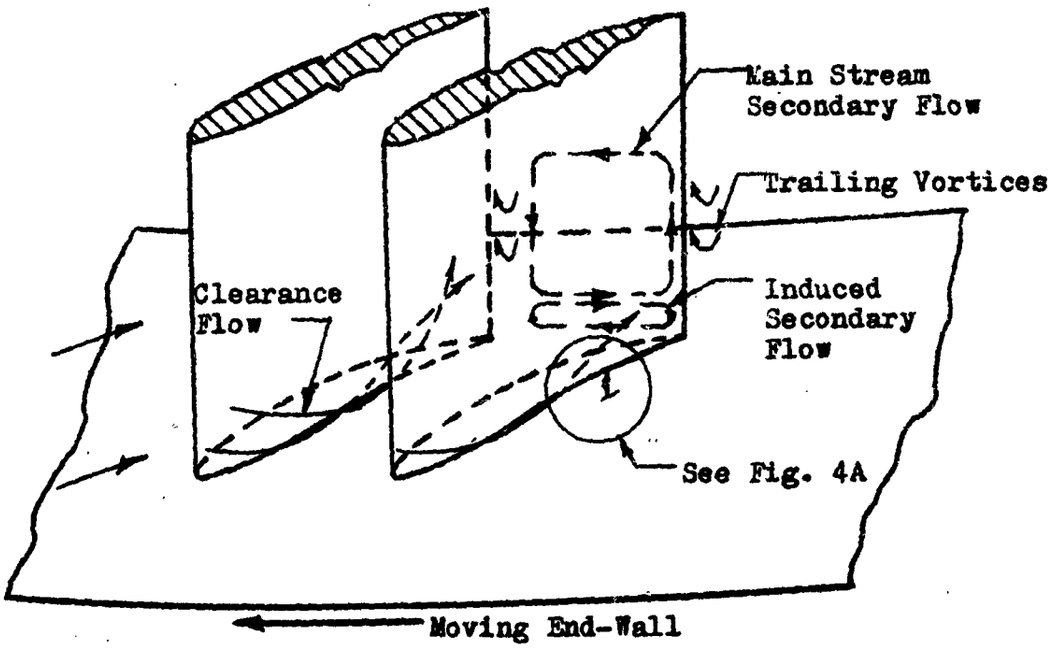

FIG. 4 - Flow Past Blades With Moving End-Wall And Tip-Clearance in a Compressor.

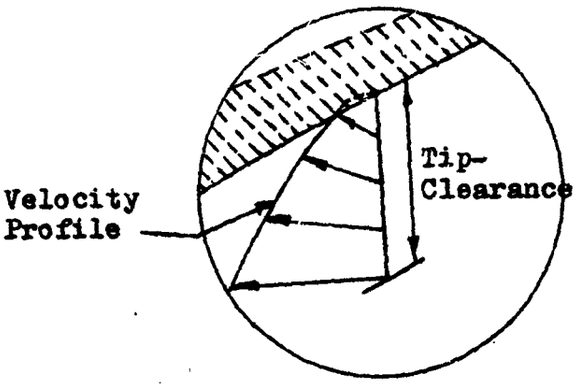

FIG. 4A - Details of Flow Inside Clearance Space

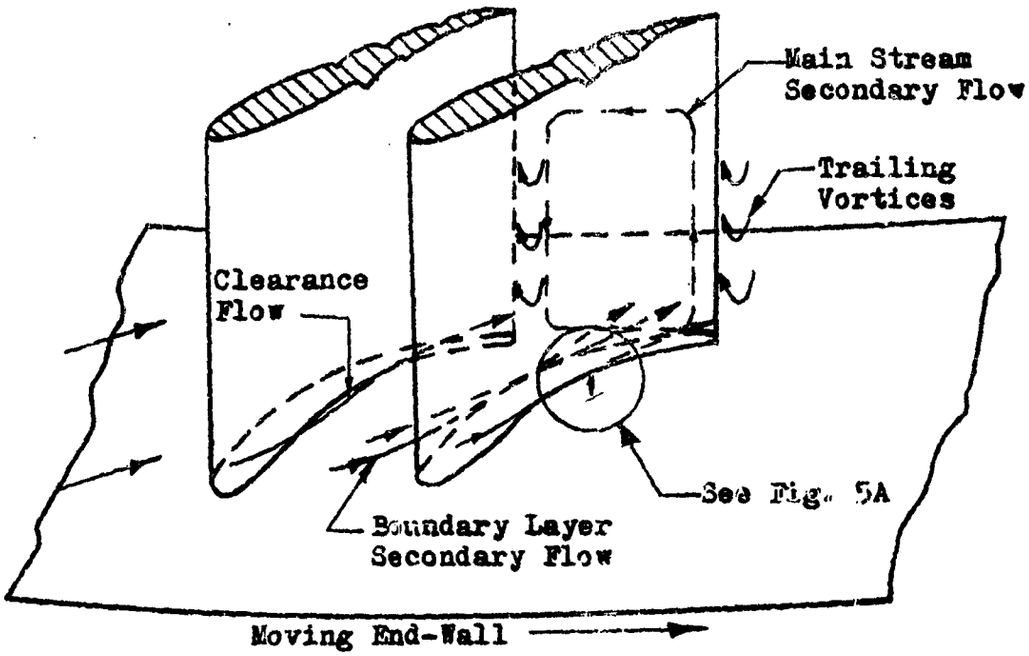

FIG. 5 - Flow Past Blades With Moving End-wall And Tip-Clearance in a Turbine.

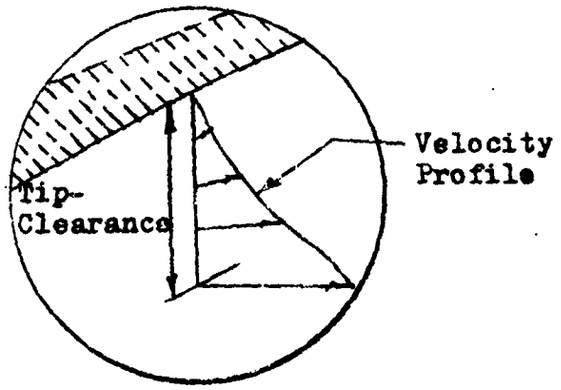

FIG. 5A - Details of Flow Inside Clearance Space.

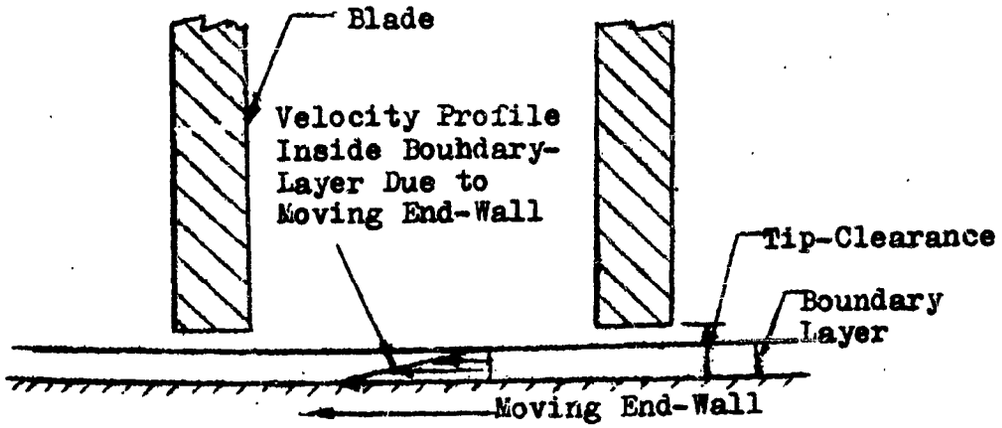

FIG. 6 - Blade Tips Outside of End-Wall Boundary Layer.

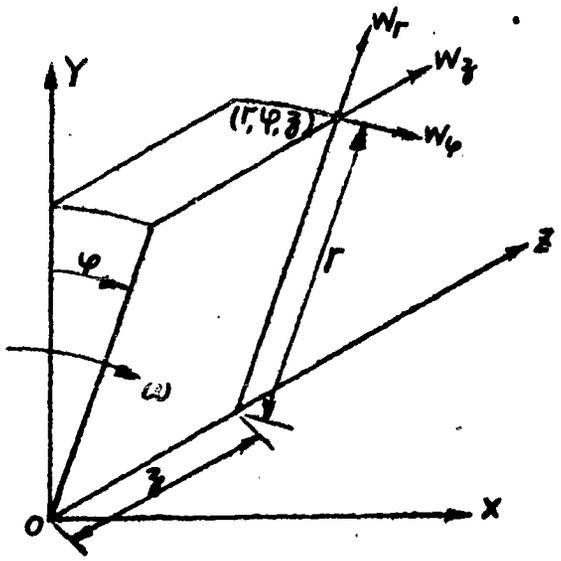

FIG. 7 - Rotating Cylindrical Coordinates.

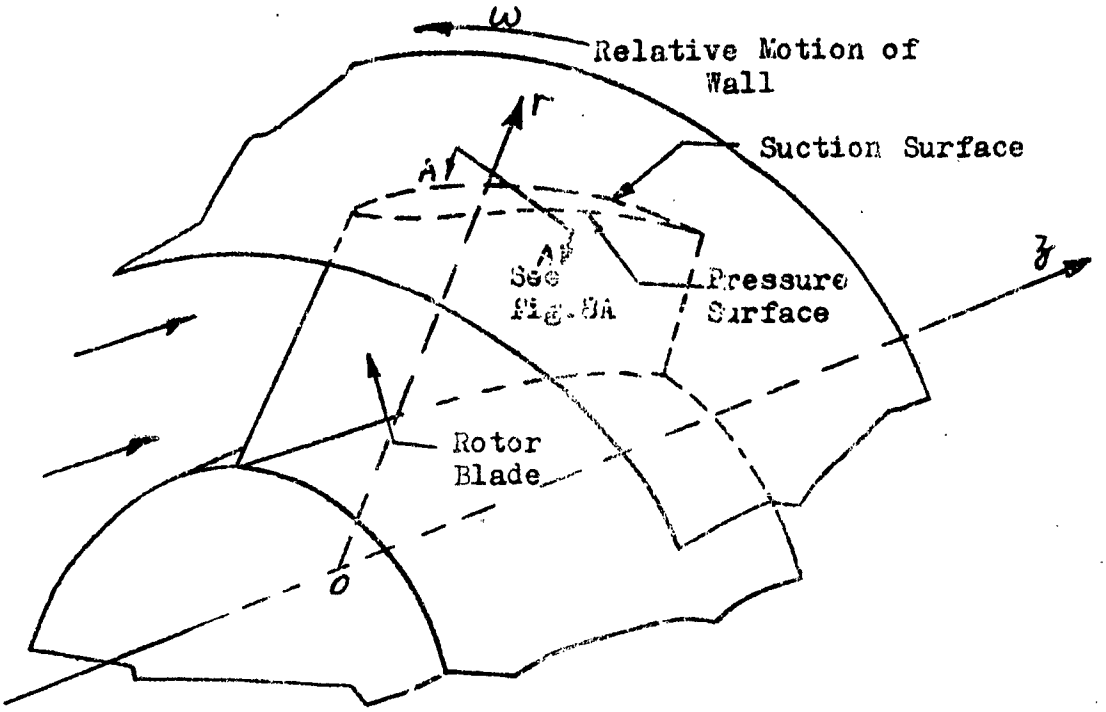

FIG. 8 - Relative Motion of Compressor Rotor.

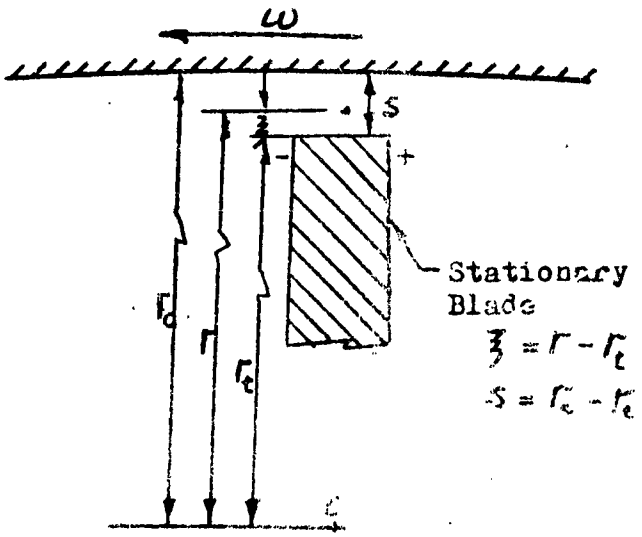

FIG. 8A - Cross-Section A-A.

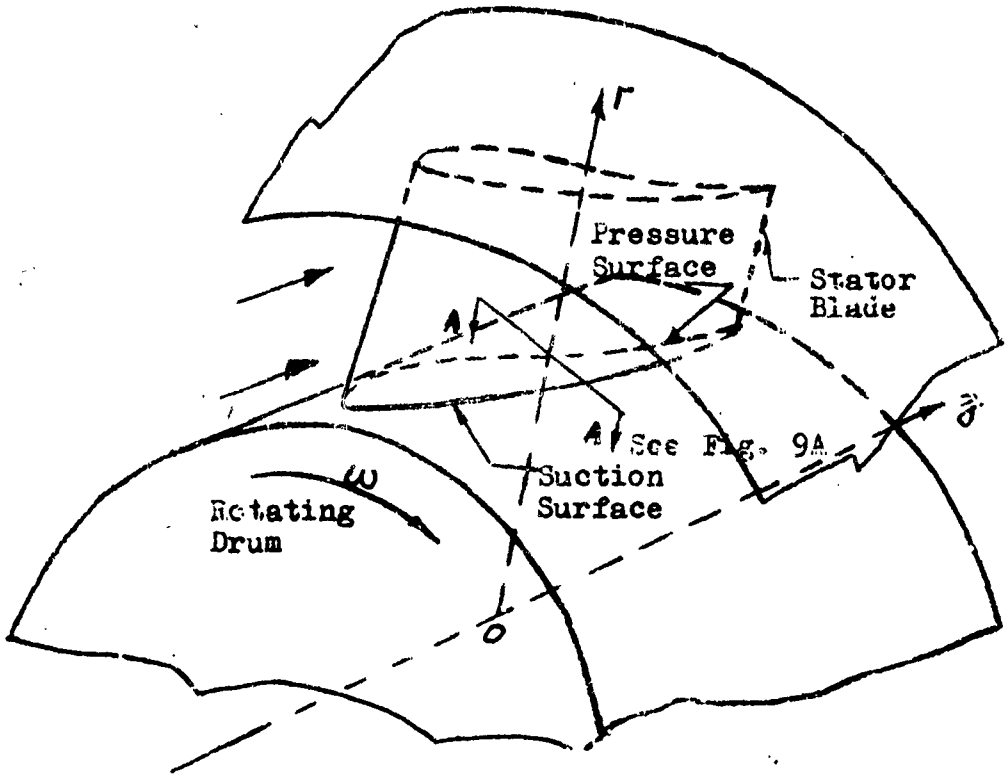

FIG. 9 - Relative Motion of Compressor Stator.

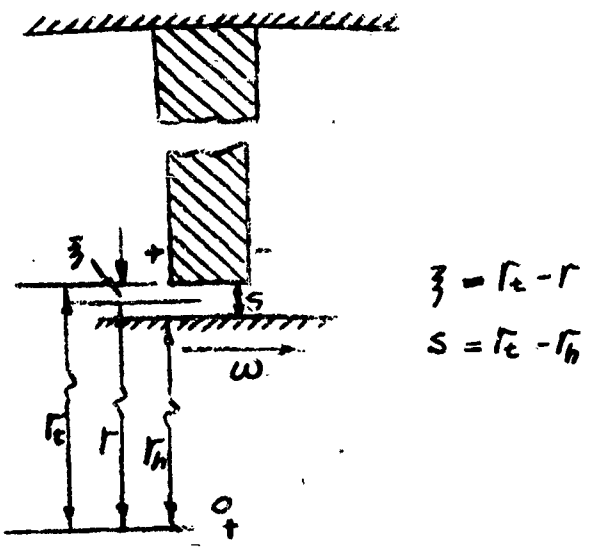

FIG. 9A - Cross-Section A-A.

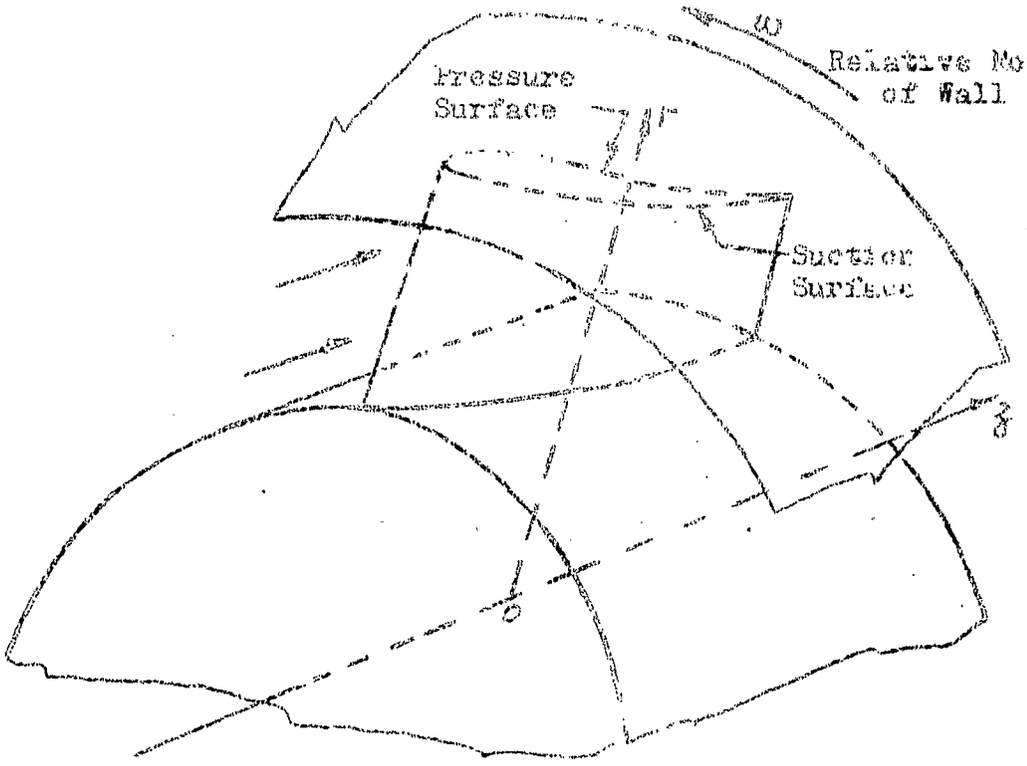

FIG. 10 - Relative Motion of Rotating Rotor.

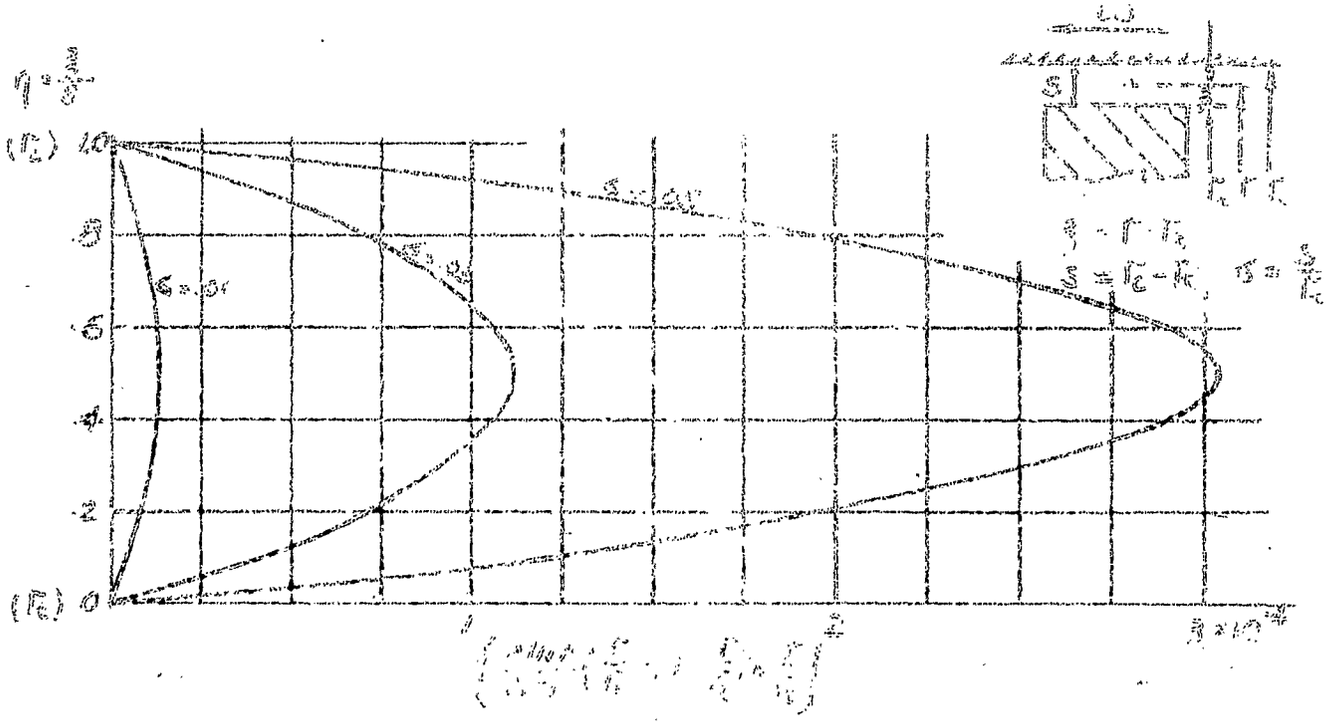

FIG. 11 - Variation of Coefficient of Pressure Gradient Inside Rotor Tip Clearance Space.

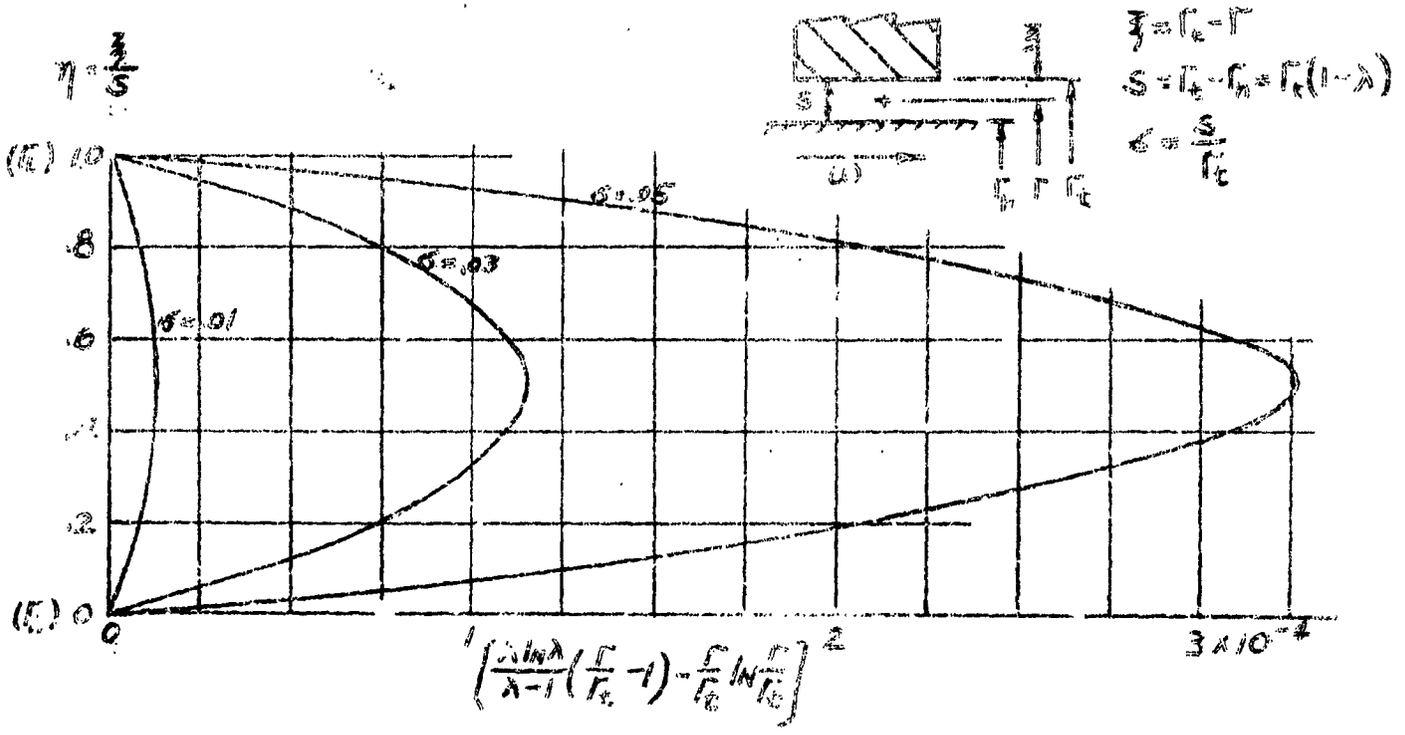

FIG. 12 - Variation of Coefficient of Pressure Gradient Inside Stator Tip Clearance Space.

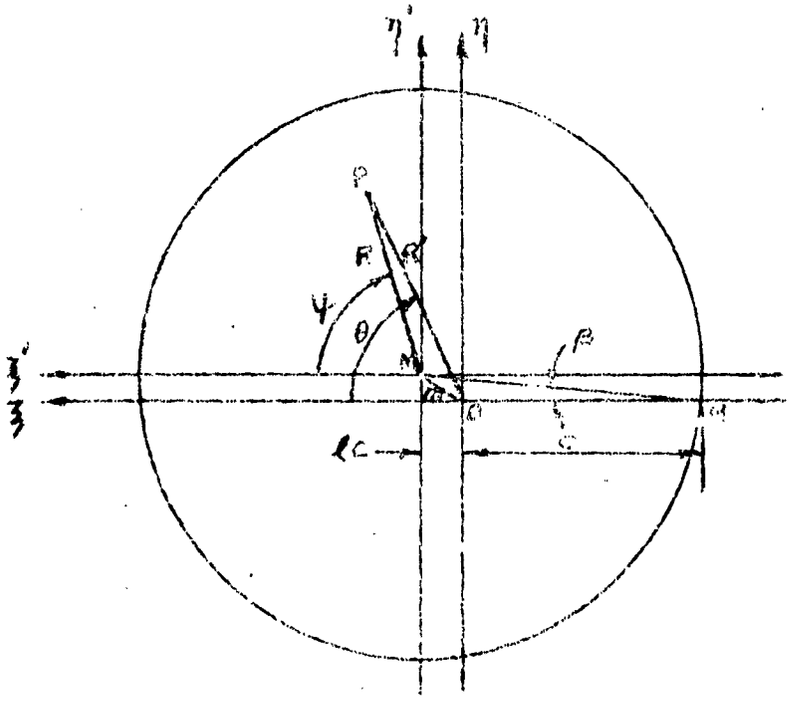

FIG. 14 - Polar Coordinates R and ψ for Solution of Pressure Distribution.

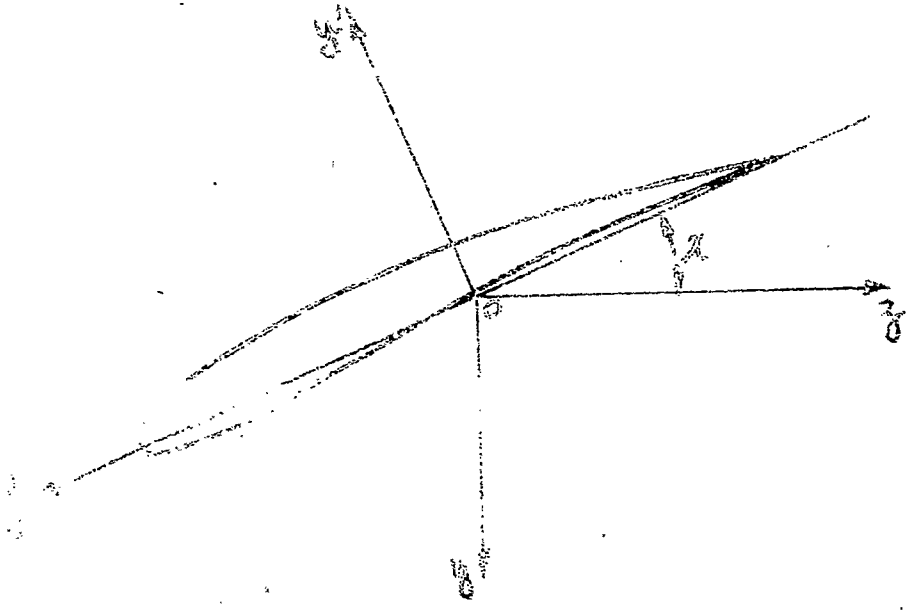

FIG. 13A - Joukowsky Airfoil in y-z Plane

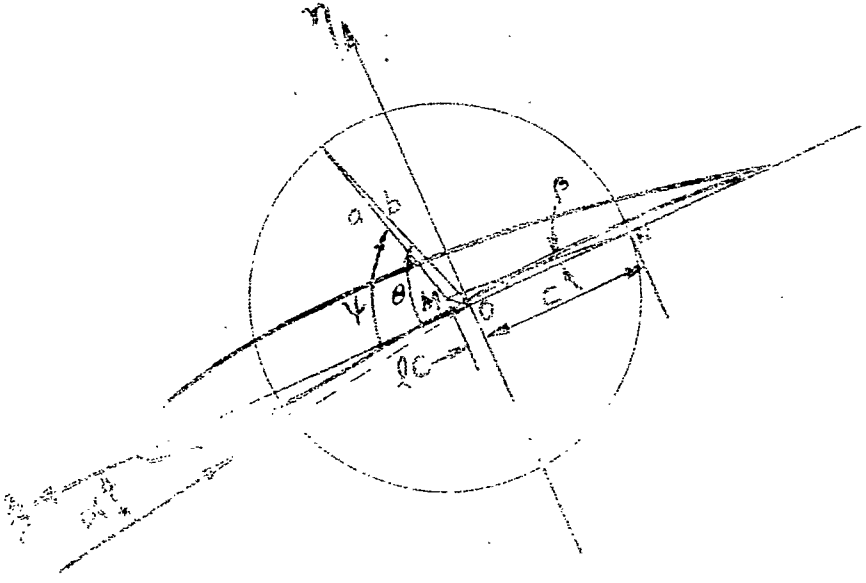

FIG. 13B - Joukowsky Airfoil Transformed into A Circle in ζ Plane

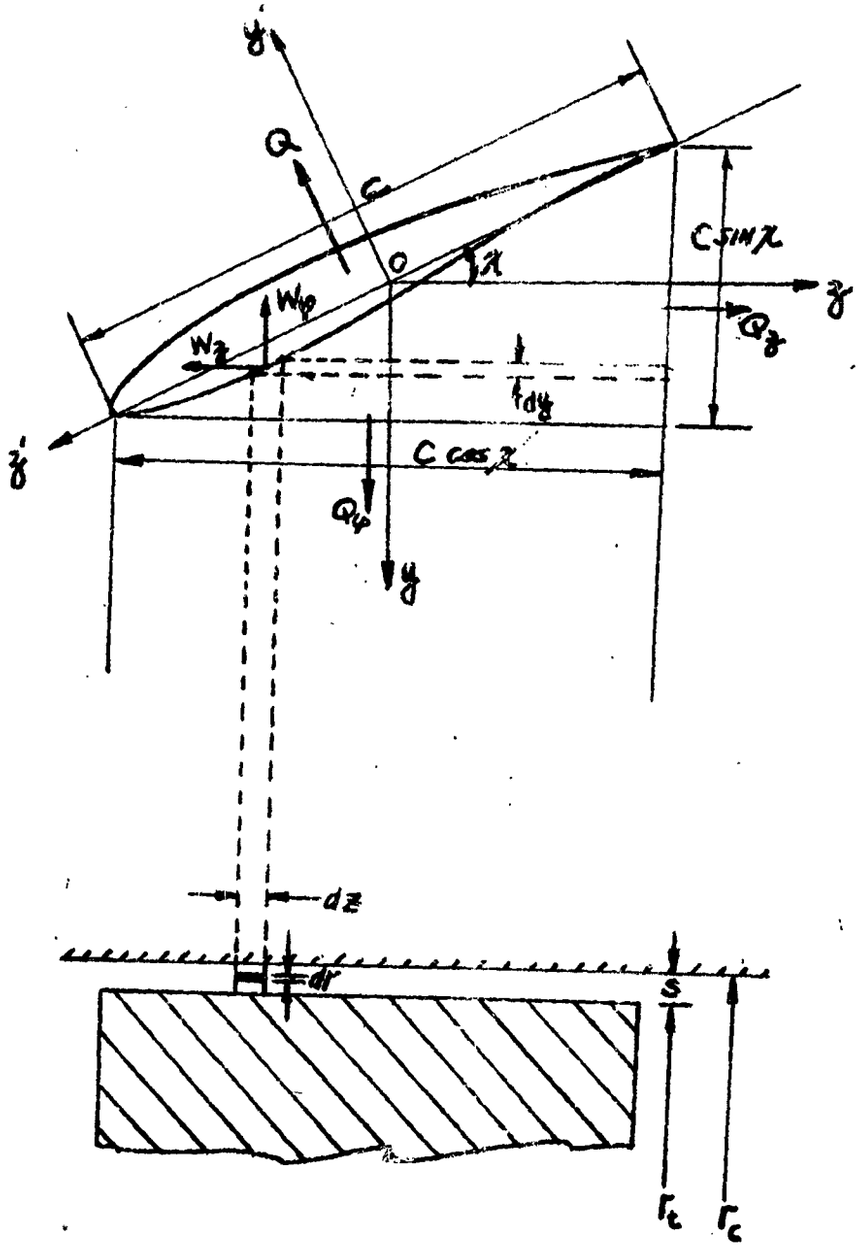
y
Q
C
O
χ
C SIN χ
z
W_φ
W_z
Q_z
f_{dy}
C cos χ
Q_φ
y
z
dz
dr
s
r_t
r_c

APPROVED DISTRIBUTION LIST FOR

UNCLASSIFIED TECHNICAL REPORTS ISSUED UNDER

CONTRACT Nonr 83904

PROJECT NR 062-172

Encl (1)

Chief of Naval Research
Department of the Navy
Washington 25, D. C.
Attn: Code 438 (2)

Commanding Officer
Office of Naval Research
Branch Office
150 Causeway Street
Boston, Massachusetts (0)

Commanding Officer
Office of Naval Research
Branch Office
The John Crerar Library Bldg.
86 East Randolph Street
Chicago 1, Illinois (1)

Commanding Officer
Office of Naval Research
Branch Office
346 Broadway
New York 13, New York (2)

Commanding Officer
Office of Naval Research
Branch Office
1030 East Green Street
Pasadena, 1, California (1)

Commanding Officer
Office of Naval Research
Branch Office
1000 Geary Street
San Francisco, 24, California (1)

Commanding Officer
Office of Naval Research
Navy #100, Fleet Post Office
New York, New York (3)

Director
Naval Research Laboratory
Washington 25, D. C.
Attn: Code 2021 (6)

Documents Service Center
Armed Services Technical
Information Agency
Knott Building
Dayton 2, Ohio (5)

Chief Bureau of Aeronautics
Department of the Navy
Washington 25, D. C.
Attn: Research Division (1)

Chief, Bureau of Ordnance
Department of the Navy
Washington 25, D. C
Attn: Research and Development
Division (1)

Office of Ordnance Research
Department of the Army
Washington 25, D. C. (1)

Commander
Air Research and Development Command
Office of Scientific Research
P. O. Box 1395
Baltimore 18, Maryland
Attn: Fluid Mechanics Division (1)

Director of Research
National Advisory Committee
for Aeronautics
1724 F Street, Northwest
Washington 25, D. C. (1)

Director
Langley Aeronautical Laboratory
National Advisory Committee
for Aeronautics
Langley Field, Virginia (1)

Director
National Bureau of Standards
Washington 25, D. C.
Attn: Fluid Mechanics Section (1)

Professor R. Courant
Institute for Mathematics and
Mechanics
New York University
45 Fourth Avenue
New York 3, New York (1)

Professor G. Kuerti
Department of Mechanical
Engineering
Case Institute of Technology
Cleveland, Ohio (1)

Professor W. R. Sears, Director
Graduate School of Aeronautical
Engineering
Cornell University
Ithaca, New York (1)

Chief, Bureau of Yards and Docks
Department of the Navy
Washington 25, D. C.
Attn: Research Division (1)

Director
Underwater Sound Laboratory
Fort Trumbull
New London, Connecticut (1)

Director
Waterways Experiment Station
Box 631
Vicksburg, Mississippi (1)

Office of the Chief Engineers
Department of the Army
Gravelly Point
Washington 25, D. C. (1)

Beach Erosion Board
U. S. Army Corps of Engineers
Washington 25, D. C. (1)

Commissioner
Bureau of Reclamation
Washington 25, D. C. (1)

Dr. G. H. Keulegan
National Hydraulic Laboratory
National Bureau of Standards
Washington 25, D. C. (1)

Professor V. L. Streeter
Civil Engineering Department
University of Michigan
Ann Arbor, Michigan (1)

Chief, Bureau of Ships
Department of the Navy
Washington 25, D. C
Attn. Research Division (1)

Commander
Naval Ordnance Test Station
3202 E. Foothill Boulevard
Pasadena, California (1)

Commanding Office and Director
David Taylor Model Basin
Washington 7, D. C.
Attn: Hydromechanics Lab. (1)
Hydromechanics Div. (1)
Library (1)

California Institute of
Technology
Hydrodynamic Laboratory
Pasadena 4, California (1)

Commanding General
Arnold Engineering Development
Center
P. O. Box 162
Tullahoma, Tennessee
Attn: Library (1)

Commanding Officer and Director
David Taylor Model Basin
Washington 7, D. C.
Attn: Ship Division (1)

Hydrographer
Department of the Navy
Washington 25, D. C. (1)

Professor V. A. Vanoni
Hydrodynamics Laboratory
California Institute of Technology
Pasadena 4, California (1)

Professor M. L. Albertson
Department of Civil Engineering
Colorado A & M College
Fort Collins, Colorado (1)

Professor H. A. Thomas
Pierce Hall
Harvard University
Cambridge 38, Massachusetts (1)

Dr. F. N. Frenkiel
Applied Physics Laboratory
Johns Hopkins University
8621 Georgia Avenue
Silver Spring, Maryland (1)

Professor A. T. Ippen
Hydrodynamics Lanoratory
Massachusetts Institute of
Technology
Cambridge 39, Massachusetts (1)

Dr. R. R. Revelle
Scripps Institute of Oceanography
La Jolla, California (1)

Professor J. K. Vennard
Department of Mechanical Engineering
Stanford University
Standford, California (1)

Dr. Hunter Rouse, Director
Iowa Institute of Hydraulic
Research
State University of Iowa
Iowa City, Iowa (1)

Stevens Institute of Technology
Experimental Towing Tank
711 Hudson Street
Hoboken, New Jersey (1)

Professor J. W. Johnson
Fluid Mechanics Laboratory
University of California
Berkeley 4, California (1)

Professor H. A. Einstein
Department of Engineering
University of California
Berkeley 4, California (1)

Professor J. R. Weske
Institute for Fluid Dynamics
and Applied Mathematics
University of Maryland
College Park, Maryland (1)

Dr. L. G. Straub
St. Anthony Falls Hydraulic
Laboratory
University of Minnesota
Minneapolis 14, Minnesota (1)

Dr. G. H. Hickox
Engineering Experiment Station
University of Tennessee
Knoxville, Tennessee (1)

Director
Woods Hole Oceanographic
Institute
Woods Hole, Massachusetts (1)

Mr. C. A. Gongwer
Aerojet General Corporation
6352 N. Irwindale Avenue
Azusa, California (1)

Chief Bureau of Ordnance
Department of the Navy
Washington 25, D. C.
Attn: Code Re6a (1)

Chief Bureau of Ships
Department of the Navy
Washington 25, D. C.
Attn: Ship Design Division (1)
Prop & Shafting Branch (1)

Commanding Officer
Naval Ordnance Laboratory
White Oak, Maryland
Attn: Underwater Ordnance
Department (1)

Commanding Officer
Naval Torpedo Station
Newport, Rhode Island (1)

Commanding Officer and Director
David Taylor Model Basin
Washington 7, D. C.
Attn: Ship Division (1)

Director
Lewis Flight Propulsion Laboratory
National Advisory Committee
for Aeronautics
21000 Brookpark Road
Cleveland 11, Ohio

Professor C. H. Wu
Department of Mechanical Engineering
Polytechnic Institute of Brooklyn
99 Livingston Street
Brooklyn 2, New York (1)

Professor H. Reissner
Department of Aeronautical
Engineering and Applied Mechanics
Polytechnic Institute of Brooklyn
99 Livingston Street
Brooklyn 2, New York (1)

Professor P. F. Maeder
Division of Engineering
Brown University
Providence 12, Rhode Island (1)

Professor D. Rannie
Department of Mechanical Engineering
California Institute of Technology
Pasadena 4, California (1)

California Institute of Technology
Hydrodynamics Laboratory
Pasadena 4, California
Attn: Professor A. Hollander (1)
Professor R. T. Knapp (1)
Professor M. S. Plesset (1)

Professor G. F. Wislicenus
Department of Mechanical Engineering
John Hopkins University
Baltimore 18, Maryland (1)

Massachusetts Institute of Technology
Department of Naval Architectures
Cambridge 39, Massachusetts (1)

Dr. J. M. Robertson
Ordnance Research Laboratory
Pennsylvania State University
State College, Pennsylvania (1)

Dean K. E. Schoenherr
College of Engineering
University of Notre Dame
Notre Dame, Indiana (1)

Professor J. L. Hooper
Alden Hydraulic Laboratory
Worcester Polytechnic Institute
Worcester, Massachusetts (1)

Director
Jet Propulsion Laboratory
California Institute of Technology
Pasadena 4, California (1)

Professor J. V. Charyk
Forrestal Research Center
Princeton University
Princeton, New Jersey (1)